ELSEVIER

Contents lists available at ScienceDirect

# International Journal of Heat and Mass Transfer

journal homepage: www.elsevier.com/locate/hmt



# A comprehensive approach to the mathematical modeling of mass transport in biological systems: Fundamental concepts and models\*



Shadi Zaheri, Fatemeh Hassanipour\*

Department of Mechanical Engineering, The University of Texas at Dallas, Richardson, TX, 75080, USA

#### ARTICLE INFO

Article history: Received 17 December 2019 Revised 14 March 2020 Accepted 8 April 2020 Available online 30 June 2020

Keywords:
Biological transport mechanism
Membrane transporter
Mass transport in Tissue's comportment
Mathematical modelling
Flow transport in biological systems

#### ABSTRACT

Multiscale mathematical modeling of transport phenomena across different levels of biological systems, such as cells, capillaries, tissues, and organs, has been increasingly helpful in describing how interactions among these systems lead to their function and dysfunction. The development of models across these scales is based on knowledge from various fields, such as engineering, physiology, and biophysics, and it requires significant collaboration among scientists from the relevant areas. Therefore, a unified framework to describe the fundamental principles and unite the established models could support this growing research community. In this regard, the present work deals with the essential terminology required to understand and model biological transport mechanisms, as well as to compile currently available models. An inclusive mathematical framework for models of mass transport mechanisms in different tissue compartments, including cells, capillaries, and gland ducts, is developed, with a primary focus on the mechanisms of membrane-mediated transporters such as channels, uniporters, symporters, pumps, and antiporters. The main objective of this study is to provide a comprehensive tool to facilitate the analysis of biological mass transport mechanisms and substantially decrease the time taken to find the appropriate model for a study.

© 2020 Elsevier Ltd. All rights reserved.

## 1. Introduction

Mass transport mechanisms in complex biological systems, such as cells, tissues, and organs, are tightly regulated; any dysregulation can result in diseases, such as membrane disorders, cancer, and other complex diseases. It is necessary to understand the relationships among transport mechanisms in different biological systems and to be able to predict their behavior under various conditions. Mathematical and computational modeling are powerful tools to describe the interactions that occur at the different levels of biological systems and to predict tissue and organ behavior under different conditions. Researchers have used mathematical models extensively to understand the diseases caused by perturbations in biological transport processes [1-9]. Interest in this area of research has grown rapidly, with many published examples demonstrating the importance of these models in the analysis of transport processes and transport-related disorders. This progress has been enabled by the coupling of experimental and computational

E-mail addresses: shadi.zaheri@utdallas.edu (S. Zaheri), fatemeh@utdallas.edu (F. Hassanipour).

studies at multiple scales and cooperation among researchers from different backgrounds.

Numerous mathematical models have been provided in chapters of books in the fields of biology, physiology, and engineering [10–26] as well as in research articles dealing with the neurological system [27,28], cardiovascular system [29–32], respiratory system [33,34], cellular level behavior [35–38], nutrient transport [39], and membrane transporters and channels [40–42], among others.

However, there is a need to gather and examine the work that has been done previously in order to develop an outline of the further work required to make these models more practical and improve the quality of their predictions. Furthermore, consolidating all the models into one framework will provide researchers with access to better alternative fitting models for different experimental/clinical analyses. In many cases, transport models that are invalid for the given operating conditions are used simply because of the lack of a better alternative model. For example, in several instances, movements of some molecules across the membrane may be assumed to happen with the constant rate, simply because of not having the relevant model describing the molecule movement through the membrane-transporters available. With collecting all the models unitedly, including those categorized based on the types of membrane transporters, there is a possibility to obtain extremely more accurate model information for the mass transport

 $<sup>\,^{\</sup>star}\,$  This document is the results of the research project funded by the National Science Foundation.

<sup>\*</sup> Corresponding author.

Nomenclature	
Square brackets:	Typically are used with letters (e.g., [A], [B], [EA]) to indicate the concentration of the substrate.
Subscripts E and compounds (e.g., EA, EB, EAB):	When used with reaction or transport quantities (e.g., reaction rate constants, translocation rate, concentration, flux), these refer to carrier and to the carrier-substrate complex, re-
Subscripts i, A, B, and C:	spectively. When used with reaction or transport quantities (e.g., reaction rate constants, concentration, flux), these refer to solute
Superscripts M and N:	'i', 'A', 'B', and 'C', respectively. When used with reaction or transport quantities (e.g., concentration, flux), these refer to the transport domain in a sys-
F	tem with multiple domains. Faraday's constant 96,490
$K_B$	(A · s/mol) Boltzmann's constant $1.38 \times 10^{-23} \ (m^2 \cdot kg/(s^2 \cdot K))$
R	Universal gas constant 8.314 $(J/(mol \cdot K))$
$eta_i$	Restriction coefficient of a solute 'i'
$\Delta$ $\eta_h$ $\gamma^M$ $\hat{v}_s$ $\Lambda_i^{\infty}$ $\mu$	Operator to describe the change of any changeable quantity (e.g., $\Delta \pi^{M,N}$ is osmotic pressure difference between M and N domains) Hill coefficient Ratio of the surface area of compartment M to tissue volume Molar volume of the solute Electrical conductance of ion 'i' in the solution Dynamic fluid viscosity Operator to either get the gradient tensor of a vector, the divergence of a vector or to find the gradient of a scalar field
$\pi$ $\Pi$ $\psi$ $\rho$ $\sigma(y)$ $\sigma_i$ $\sigma_p(y)$ $\tau$ $\varepsilon$ $\varepsilon^M$	Osmotic pressure Oncotic pressure Electrical potential Fluid density Local charge density Reflection coefficient of a solute 'i' through the membrane Charge density on the immobilized protein wall of the membrane channel Tortuosity coefficient Porosity of the wall Ratio of the volume faction occupied by compartment M to the tissue volume
$arepsilon_0$	Dielectric constant Solvent association factor

u	Fluid velocity
<del>u</del>	Averaged fluid velocity
$\overline{C_i}$	Volume-averaged molar concen-
M N	tration of species 'i'
$\overline{C_i}^{M,N}$	Logarithmic mean average of the
	molar concentrations at the two
	sides of the membrane
$\overline{R_i}$	Volumetric reaction rate of so-
1	lute 'i'
E	Electric field
E	
$A_p$	Available area of the heteroge-
	neous porous membrane
$a_p$	Radius of the membrane pores
$A_s$	Surface area of the tube
$a_{s}$	Radius of the spherical
	molecule/solute
$a_t$	Tube radius
$C_i$	Molar concentration of species
C <sub>1</sub>	'i'
C	-
$C_L$	The concentration of unbound
	ligand for the Hill model
$D_{i}$	Diffusion coefficient of species 'i'
$f_0^{channel}$	Open probability of the ion
	channel
F <sub>convection</sub>	Axial volumetric convection fluid
Convection	flow rate in the tube
For	Volumetric filtration fluid flow
F <sub>filtration</sub>	rate
~	
g	Translocation rate constant
gi,channel	Membrane conductance for
	channels of ion $'i'$ (channel
	conductance)
I'' i,channel	Net current density of ion 'i'
i, chamici	through the ion channels
I	The transported flux driven via
Jantiporter	antiporters
7	
JATPase	The transported flux driven via
_	ATPase pumps
J <sub>filtration</sub>	The transported flux due to the
	hindered convection
Ji, convection	Molar flux of solute 'i' by con-
•	vection
J <sub>i,diffusion</sub>	Molar flux of solute 'i' by diffu-
J i, aij jusion	sion
1	Molar flux of solute 'i' by migra-
J <sub>i,migration</sub>	
-M	tion
$J_{i,wall}^{M}$	The net outward molar flux of
	solute 'i' from domain 'M' across
	the wall
Jionchannel	The ion flux through the ion
ronenamer	channels
Jsymporter	The transported flux driven via
Jsymporter	symporters
7	
Juniporter	The transported flux driven via
_	uniporters
Jwaterchannel	The water flux through the wa-
	ter channels
K	When used in the carrier-
	mediated transport equa-
	tions (e.g., $K_A^M = k_A^{-M}/k_A^{+M}$ ,
	$VM = I_A - I_A / I_A$
	$K_B^M = k_B^{-M}/k_B^{+N}$ ), it indicates
	the dissociation constant for a
	reaction step.

$k^+$	Binding rate constant (e.g., $k_A^+$ is
	the binding constant for solute
$k^-$	A) Unbinding rate constant (e.g., $k_A^-$
	is the unbinding constant for so-
	lute A)
$K_A$	The ligand concentration at which half-saturation is
	achieved, for Hill model
$K_i^M$	Equilibrium constant coefficient
1	for substrate 'i' in domain M
K <sub>m</sub>	Michaelis-Menten rate constant,
	which is the substrate concen-
	tration at half the maximum
	rate $(V_{\text{max}})$
$K_i^m$	Membrane partition coefficient for solute 'i'
$L_{ m p}^{ m waterchannel}$	Hydraulic conductivity of the
P	water channel
$L_p$	Hydraulic conductivity (filtration
	coefficient) of the membrane
$l_t$	Tube Length
M <sub>W</sub>	Molecular weight of the solvent
O <sup>channel</sup>	The total number of open chan-
	nels per unit area of the mem- brane
P	Hydraulic pressure
$P_i^m$	Membrane permeability coeffi-
1	cient to the solute 'i'
T	Temperature
$t_m$	Membrane thickness
$u_{wall}$	Transmembrane fluid flow
$V_m$	Membrane voltage or membrane
V	electric potential
$V_{i, rev}$	Membrane reversal potential for a single ion 'i'
$V_{ m max}$	Maximum reaction velocity
· IIIdA	achieved at the saturated sub-
	strate concentrations for the
	Michaelis-Menten model
$z_i$	Ionic charge number on an ion
	'i'

mechanisms that are of interest to us. Another challenge in the area of multiscale transport modeling of biological systems is the lack of common language among researchers from relevant fields. This study aims to provide an interface for researchers from different fields with interest in the area of biological transport mechanisms. In this regard, the present work integrates engineering principles with relevant physiological, biophysical, and biomedical concepts and defines the essential terminology from the relevant fields. To accomplish this, a full review of mass transport models within and across individual biological systems, including capillaries, the interstitial region, cell membranes, intracellular regions of the cell, and duct lumina, has been performed. First, the essential concepts of continuity, transport, and the relevant kinetic equations and their connection to solute distribution in biological systems are outlined in Sections 2 and 3. Next, a detailed discussion of the three main transport mechanisms, namely, convection, diffusion, and migration, is provided in Sections 4.1, 4.2, and 4.3. An application of these models to different types of membrane-mediated transport mechanisms, including channels and carriers, along with the relevant kinetic equations, is described in Sections 5.1 and 5.2. Detailed kinetic modeling approaches for membrane transporters are described without emphasizing any particular family. For each family of membrane transporters, most of the previously published models are presented and transformed into a general identical parametric form. Furthermore, our review of previously published models prompted us to derive some new kinetic models for membrane-transporter mechanisms. This work does not attempt to evaluate or analyze these models, but instead intends to provide a comprehensive modeling toolbox that should facilitate investigation of membrane transport mechanisms.

#### 2. Model construction

Biological systems can be categorized into different levels, ranging from cells and the interstitial region to capillaries, tissues, and organs. For a living biological system to operate, nutrients and other molecules must continuously move across the boundaries of the system at each level and participate in biochemical reactions.

In this work, a heterogeneous representative elementary volume (REV) is used to represent the tissue at a macroscopic scale (Fig. 1). Next, at the microscopic scale, each of the tissue compartments, including the cell, interstitial, and capillary phases, is considered as an individual control volume (CV), and the transport processes of fluids (solutions such as blood and air) and solutes (such as nutrients, hormones, electrolytes, oxygen, and carbon dioxide) across the boundaries of these control volumes is modeled.

The models of volume-averaged fluid flow and solute transport (through the regions "M" and "N") within the defined control volumes are shown in Fig. 2. For the purpose of simplification, it is assumed that the flow is incompressible, laminar, Newtonian, and that there is no fluid accumulation in the boundaries.

The macroscopic mass and momentum continuity equations for mass transport through regions "M" and "N" are as follows [43,44]:

$$\nabla . \tilde{\mathbf{u}} = 0 \tag{1}$$

$$\frac{\partial \overline{\mathbf{u}}^{M}}{\partial t} + \overline{\mathbf{u}}^{M} \cdot \nabla \overline{\mathbf{u}}^{M} = \frac{1}{\rho} \left( \mu^{M} \nabla^{2} \overline{\mathbf{u}}^{M} - \nabla \overline{P}^{M} \right)$$
 (2)

Where  $\mathbf{u}^M$  is the fluid velocity in region M,  $\rho$  is the fluid density,  $\nabla P^M$  is the pressure drop along the tube, and  $\mu$  is the dynamic fluid viscosity.

The microscopic form of the Navier-Stokes and mass-momentum conservation equations and the corresponding dynamic fluid flow model can be expressed using the equations below [45–48]:

$$\overline{\nabla . \mathbf{u}^{\mathbf{M}}} = \nabla . \overline{\mathbf{u}}^{\mathbf{M}} + \frac{\gamma^{\mathbf{M}}}{\varepsilon^{\mathbf{M}}} u_{wall}^{\mathbf{M}} = 0 \quad \Rightarrow \quad \nabla . \overline{\mathbf{u}}^{\mathbf{M}} = -\frac{\gamma^{\mathbf{M}}}{\varepsilon^{\mathbf{M}}} u_{wall}^{\mathbf{M}}$$
(3)

$$\rho \left( \frac{\partial \overline{\mathbf{u}}^{M}}{\partial t} + \overline{\mathbf{u}}^{M} \cdot \nabla \overline{\mathbf{u}}^{M} \right) = -\nabla \overline{P}^{M} + \mu^{M} \nabla^{2} \overline{\mathbf{u}}^{M} 
\Rightarrow \frac{\partial \overline{\mathbf{u}}^{M}}{\partial t} = -\overline{\mathbf{u}}^{M} \cdot \nabla \overline{\mathbf{u}}^{M} + \frac{1}{\rho} \left( \mu^{M} \quad \nabla^{2} \overline{\mathbf{u}}^{M} - \nabla \overline{P}^{M} \right)$$
(4)

Where  $\gamma^M$  is the ratio of the surface area of compartment M to tissue volume and  $\varepsilon^M$  is the ratio of the constant volume occupied by compartment M to the tissue volume (volume fraction). The product  $\gamma^M$   $u^M_{wall}$  represents the volumetric solution outflow per unit tissue volume through the boundary of compartment M.

Similarly, the volume-averaged continuity equations of the solute 'i' on the macroscopic scale (Eq. (5)) and microscopic scale (Eq. (6)) govern the distribution of the molar concentration of the solute [49,50].

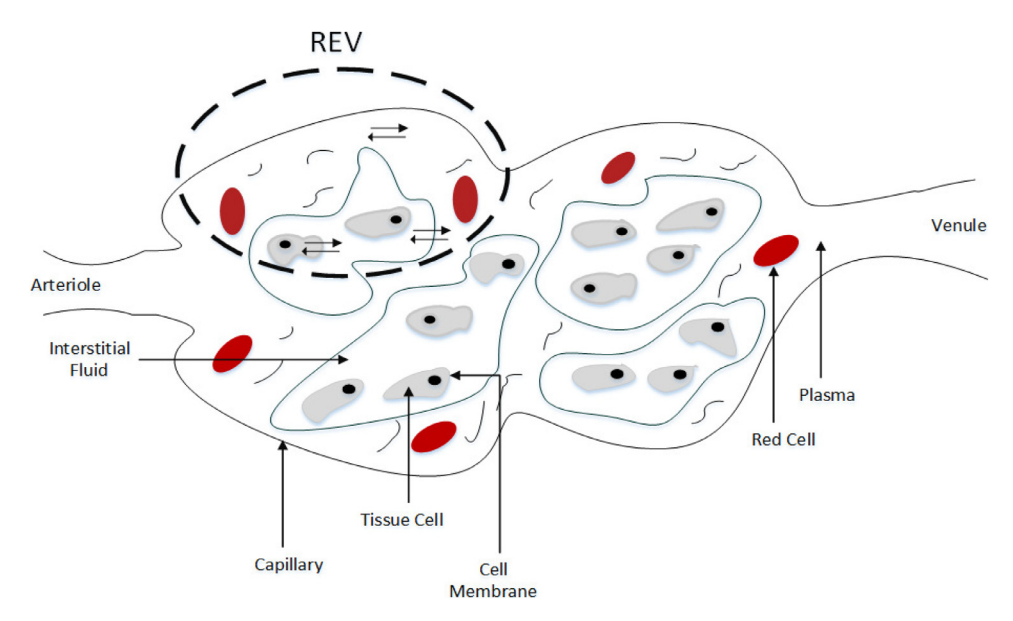
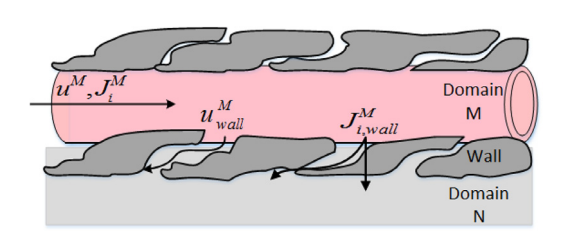


Fig. 1. Representative Elementary Volume (REV) of a general tissue consists of capillary, interstitial fluid, and cells.



**Fig. 2.** Volumetric fluid movement within a control volume  $(u^M)$  and the transmembrane flow  $(u_{wall})$ . Solute transport flux within the control volume  $(I_i^M)$  can happen by *convection*, *diffusion*, and *migration* mechanisms.  $J_{i,wall}^M$  represents the net outward molar flux of solute 'i' from control volume 'M' to its adjacent compartments across the wall (e.g., N). Transport between the M and N compartments can occur either through the gaps between the cells of the wall separating the domains (the curved arrow) or across the individual cell membranes (the straight arrow).

$$\frac{\partial \overline{C_i}}{\partial r} = \overline{R_i} - \nabla \overline{J_i} \tag{5}$$

$$\frac{\partial \overline{C}_{i}^{M}}{\partial t} = \overline{R}_{i}^{M} - \nabla . \overline{J}_{i}^{M} - \frac{\gamma^{M}}{\varepsilon^{M}} J_{i,wall}^{M}$$
(6)

Where,

 $C_i^M$  is the molar concentration of species 'i' in the control volume 'M'.  $\overline{R_i}^M$  refers to the volumetric metabolism reactions in which the

 $\overline{R_i}^{N}$  refers to the volumetric metabolism reactions in which the substrate participates (see Section 3 for more details).

 $\mathbf{J}_i^M$  is the bulk flux of species 'i' within phase M, and is discussed in Section 4.

 $\frac{Y'''}{\varepsilon^M}J_{i,wall}^M$  represents the net outward molar flux of solute 'i' from control volume 'M' to its adjacent compartments across the wall (discussed in Sections 4 and 5)

## 3. Reaction mechanism $(R_i)$ :

Cellular reactions can occur within the control volume  $(R_i^M)$  or at the surface of a separating wall  $(R_{s,i}^{M-N})$ , and can lead to the metabolism or transport of the substrate. In this study, three commonly used approaches for modeling cellular reactions are outlined. These models include the *mass action law* (Eqs. (7a) and (7b)), the *Michaelis-Menten* (Eq. (8)) and *Hill kinetics* model

(Eq. (9)), which are given below:

Mass Action Law:

$$n^{th}$$
 order kinetics:  $\overline{R}_i^M = \prod_{i=1}^j K_i^M \left(\overline{C}_i^M\right)^{\nu_i}$  (7a)

Firtst – order kinetics: 
$$\overline{R}_i^M = K^M \overline{C}^M$$
 (7b)

Michaelis – Menten equation : 
$$\overline{R_i}^M = V_{\text{max}} \frac{\overline{C_i}^M}{K_m + \overline{C_i}^M}$$
 (8)

Hill kinetics: 
$$\overline{R_i}^M = V_{\text{max}}\theta$$
 where,  $\theta = \frac{C_L^{\eta_h}}{K_A^{\eta_h} + C_I^{\eta_h}}$  (9)

The law of mass action states that the rate of a reaction is proportional to the concentrations of its reactants and products taken to the power of their stoichiometric coefficient. Eq. (7a) represents the law of mass action for a reaction with j substrates, where  $K_i^M$  is the equilibrium constant coefficient for substrate 'i' in region M,  $\overline{C}_i$  is the volume-averaged concentration of substrate 'i', and  $v_i$  is the order of the reaction relative to substrate 'i' which has a negative value for reactants and a positive value for products. In some cases, especially for complex reactions, such as reversible, parallel, and series reactions, the reaction rate can be shown in the form of the first-order kinetic (Eq. (7b)), in which the reaction rate and the substrate concentration has a linear relationship to each other [51,52].

The Michaelis-Menten equation (Eq. (8)) is one of the most effective methods for modeling single-substrate, single-product enzyme kinetics, and metabolic reactions. It relates the reaction velocity to the substrate concentration [53]. In the Michaelis-Menten equation,  $V_{\text{max}}$  represents the maximum velocity achieved by the system at the maximum (saturated) substrate concentrations, and  $K_m$  is the Michaelis-Menten constant, which represents the concentration of the substrate when the reaction velocity is equal to half the maximum velocity [54].

The Hill equation, (Eq. (9)) is commonly used to describe the dependence between the binding of smaller molecules (*ligand*, such as ions) to macromolecules (such as proteins). The term  $\theta$  in the Hill equation represents the fraction of macromolecules

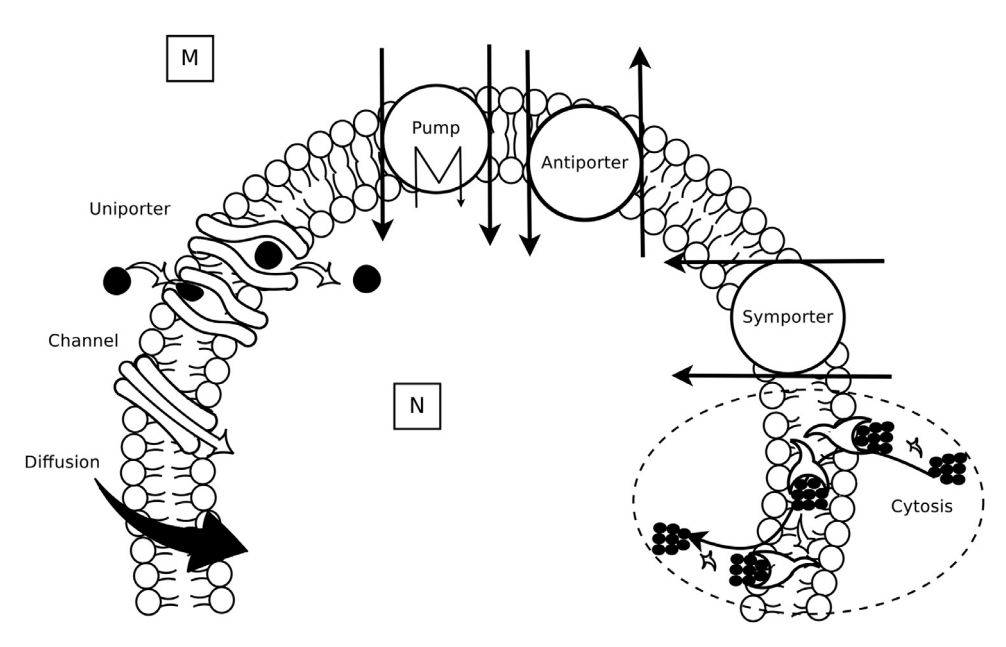


Fig. 3. Transport across the cell membrane. Movement across the cell membrane can occur through channels, including ion channels (Section 5.1.1) and water channels (Section 5.1.2), uniporters (Section 5.2.1), pumps (Section 5.2.2), symporters (Section 5.2.3), antiporters (Section 5.2.4), and cytosis.

bound to the ligand. In obtaining  $\theta$ ,  $C_L$  is the concentration of free (unbound) ligand,  $K_A$  is the ligand concentration at which half-saturation (half-activation) is achieved, and  $\eta_h$  is the Hill coefficient. The Hill coefficient is also known as the interaction coefficient, and determines the extent of cooperativity between the ligand and the macromolecule binding sites [55,56].  $\eta_h > 1$  represents positive cooperative binding,  $\eta_h < 1$  represents negative cooperative binding, and  $\eta_h = 1$  indicates a non-cooperative mechanism (completely independent binding processes). In the case of  $\eta_h = 1$  the Hill equation reduces to the familiar Michaelis Menten model ( $K_A = K_m$ ) [57].

# 4. Mass transport mechanisms:

The overall rate and type of material exchange within or across a compartment depend on the physical properties of the control volume and the structure of the separating wall, as well as the molecular features of the species being transported, such as their size, polarity, fat-solubility, diffusion coefficient, and the membrane partition coefficient for the solute.

Possible transport mechanisms "within" a control volume (e.g., M) are *convection*, *diffusion*, and *migration*, as follows:

$$\mathbf{J_{i}^{M}} = \mathbf{J}_{i,convection}^{M} + \mathbf{J}_{i,diffusion}^{M} + \mathbf{J}_{i,migration}^{M}$$
 (10)

These mechanisms and the related equations are discussed in Sections 4.1, 4.2, and 4.3, respectively.

Transport "between" the M and N domains occurs either through the gaps between the cells of the wall separating the domains or across the individual cell membranes (see Fig. 2). Mechanisms of transport through gaps between the cells include *filtration* (section 4.1) and *diffusion* (Section 4.2). Transport "across the cell membrane" can occur via diffusion, *ion channels* (Section 5.1.1), *water channels* (Section 5.1.2), *uniporters* (Section 5.2.1), *pumps* (Section 5.2.2), *symporters* (5.2.3), *antiporters* (Section 5.2.4), and *cytosis* (see Fig. 3).

The net outward molar flux across the M-N interface  $(J_i^{M,N})$  is given by:

$$\gamma^{M}J_{i,wall}^{M} = \sum_{N=1}^{m} \gamma^{M,N}J_{i}^{M,N} \tag{11}$$

Where m is the total number of adjacent control volumes. The mass transport mechanisms across the M-N wall can be grouped as follows:

$$J_{i}^{M,N} = \underbrace{J_{filtration} + J_{diffusion} + J_{ionchannel} + J_{waterchannel} + J_{uniporter}}_{passive transport} + \underbrace{J_{pump} + J_{symporter} + J_{antiporter} + J_{cytosis}}_{active transport}$$

$$(12)$$

Where.

 $J_{filtration}$  is the transported flux due to the hindered convection, and is discussed in Section 4.1,

 $J_{diffusion}$  is the transported flux due to the hindered diffusion, and is discussed in Section 4.2,

 $J_{ionchannel}$  is the ion flux through the ion channels, and is discussed in Section 5.1.1,

 $J_{water channel}$  is the water flux through the water channels, and is discussed in Section 5.1.2,

 $J_{uniporters}$  is the transported flux driven via uniporters, and is discussed in section 5.2.1,

 $J_{pumps}$  is the transported flux driven via pumps, and is discussed in Section 5.2.2,

*J*<sub>symporters</sub> is the transported flux driven via symporters, and is discussed in Section 5.2.3,

 $J_{antiporters}$  is the transported flux driven via antiporters, and is discussed in Section 5.2.4.

 $J_{cytosis}$  is the transported flux driven via cytosis mechanisms, and is not discussed in this work.

Transport mechanisms can also be categorized as passive or active transport. Passive transport (filtration, diffusion, ion channel, water channel, and uniporter mechanisms) involves the spontaneous movement of the solutes, while active transport (pump, symporter, antiporter, and cytosis) requires an external source of energy. The following sections provide a detailed discussion of all these transport mechanisms except for cytosis, as the mechanism of cytosis is entirely different from the others.

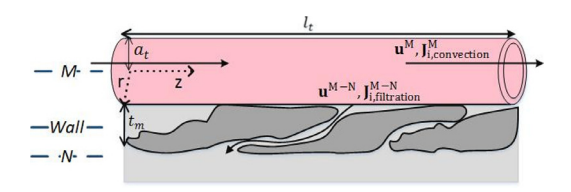


**Fig. 4.** Convective flow inside the control volume  $(\mathbf{u}^M,J_{i,convection}^M)$  and filtration flow  $(\mathbf{u}^{M-N},J_{i,filtration}^{M-N})$  through the pores across the porous wall separating the compartments.

## 4.1. Convection and filtration (J<sub>convection</sub> and J<sub>filtration</sub>):

Convection is a mass transport mechanism that occurs due to the bulk motion of the fluid within a control volume and across the semipermeable porous wall. Fluid convection can be considered at two levels: (i) Internal flow convection  $(\mathbf{u}^M,J^M_{i,convection})$ , i.e., flow within the control volume, and (ii) filtration flow  $(\mathbf{u}^{M-N},J^{M-N}_{i,filtration})$ , i.e., flow across the porous wall separating the compartments (Fig. 4).

(i) Internal flow convection (M): The Newtonian, laminar, and incompressible fluid flow inside a tube (control volume M) is governed by the Navier-Stokes and continuity equations (Eqs. (3) and (4)). A cylindrical tube whose length ( $l_t$ ) is much larger than its radius ( $a_t$ ) has no substantial radial pressure distribution, and consequently, no radial fluid movement. Under these conditions, the Poiseuille-Hagen Law relates the local "axial" fluid flow rate through a circular cross-sectional area of the tube to the hydrodynamic pressure difference at the two ends of the tube segment in the z-direction and the fluid viscosity by Loudon and McCulloh [58], Pirofsky [59], and Singh et al. [60]:

$$F_{convection}^{M}(z,t) = -\frac{\pi a_{t}^{4}}{8\mu} \frac{\partial P^{M}}{\partial z}$$
 (13)

Where  $F^M_{convection}(z,t)$  is the axial volumetric flow rate in the tube per unit time  $(cm^3/s)$ ,  $a_t=a_t(z,t)$  (cm) is the local radius of the tube,  $(\mu)$  is the fluid viscosity  $(Pa\cdot s)$ , and P=P(z,t) is the local axial pressure (Pa).

The axial fluid velocity within the tube  $(u_z^M(r))$  through the total cross-sectional area of the tube is obtained by Fournier [61] and Nield et al. [50]:

Convection – fluid: 
$$\mathbf{u}_{z}^{M}(r) = \frac{2F_{convection}}{\pi a_{t}^{4}} \left( a_{t}^{2} - r^{2} \right)$$
$$= -\frac{\left( a_{t}^{2} - r^{2} \right)}{4\mu} \frac{\partial P^{M}}{\partial z}$$
(14)

Where  $u_z^M(r)$  is a function of the radial distance from the center of the tube (0 < r <  $a_t$ ).

The convective flux of the solute,  $J_{i,convection}^{M}$  ( $mole/(s \cdot m^2)$ ), is coupled to the fluid velocity within the control volume M and the solute concentration,  $C_i^{M}$  ( $mole/m^3$ ), by Khakpour and Vafai [62] and Gösele and Alt [63]:

Convection – solute: 
$$\mathbf{J}_{i.convection}^{\mathbf{M}} = \mathbf{u}^{M} C_{i}^{M}$$
 (15)

(ii) Filtration-transmembrane flow (from M to N): Filtration involves the passage of a hindered convective flow through a porous wall, and depends on the structure of the wall and the *effective pressure difference* between the two sides of the wall. The effective pressure drop  $(\Delta P_{net}^{M.N})$  is the net result of the hydrodynamic pressure difference  $(\Delta P^{M,N})$  and the osmotic pressure difference  $(\Delta \pi^{M,N})$  between the two sides of the pore opening, and is given by Eq. (16a). The osmotic pressure difference is created by the solutes that are retained from transport across the wall and is obtained through Eq. (16b) [61,64].

$$\Delta P_{net}^{M,N} = \Delta P^{M,N} - \Delta \pi_i^{M,N} \tag{16a}$$

$$\Delta \pi_i^{M,N} = RT \sum_{i=1}^n \sigma_i \Delta C_i^{M,N}$$
 (16b)

Here, R is the universal gas constant (8.314  $J/(mol \cdot K)$ ), T is the temperature in Kelvin (human body temperature is around 300.98 K), and  $\sigma_i$  is the reflection coefficient. The reflection coefficient, which is also known as the osmotic coefficient, determines the real contribution of the osmotic pressure to the fluid flux through the membrane and is independent of the solute concentration and pressure.

The total volumetric filtration *fluid* flow rate through all the pores across the porous wall can be obtained by applying Poiseuille's Law, and is expressed as follows [61,65–67]:

$$F_{filtration}^{M,N} = L_p A_s \Delta P_{net}^{M,N} \tag{17a}$$

$$\begin{split} L_P &= \frac{\varepsilon a_p^2}{8\mu\tau t_m} = \frac{n''\pi\,a_p^4}{8\mu\tau t_m} \\ where: \qquad \varepsilon &= \frac{A_p}{A}, \qquad A_P = n\pi\,a_p^2 \qquad A_s = 2\pi\,a_t l_t \end{split} \tag{17b}$$

Where  $L_p$   $(m/(s \cdot pa))$  is the filtration coefficient,  $A_s$  is the surface area of the tube, and  $\Delta P_{net}^{M.N}$  is the effective pressure difference. The filtration coefficient, which is also known as hydraulic conductivity, determines the hydraulic permeability of the porous membrane to the fluid. The filtration coefficient can be obtained through Eq. (17b), where  $\varepsilon$  is the porosity of the wall and relates the actual available area of the heterogeneous porous membrane  $(A_p)$  to its total circumferential area  $(A_s)$ , n is the number of non-uniform inert cylindrical membrane pores, n'' is the density of the pores across the membrane  $(n/A_s)$ ,  $a_p$  is the radius of the membrane pores,  $\mu$  is the dynamic viscosity of the fluid, and  $\tau$  is the tortuosity coefficient, which relates the actual available transport path to the membrane thickness,  $t_m$  [17]. In obtaining the total circumferential area  $(A_s)$ ,  $a_t$  and  $l_t$  are the radius and length of the tube, respectively.

The net outward filtrate fluid exchange velocity (filtration or ultrafiltration velocity) across the membrane ( $\mathbf{u}^{M,N}$ ) is given by Schultz et al. [68]:

Filtration – fluid: 
$$\mathbf{u}^{M,N} = \frac{F_{filtration}^{M,N}}{A_s} = L_p \left( \Delta P^{M,N} - RT \sum_{i=1}^n \sigma_i \Delta C_i^{M,N} \right)$$
(18)

Eq. (19) relates the macroscopic filtrate fluid flow velocity across the circumferential membrane area to its microscopic velocity in the membrane pores  $(\mathbf{u}_{pore}^{M,N})$  [49].

$$\mathbf{u}_{pore}^{M,N} = \left(\frac{1}{\varepsilon}\right) \mathbf{u}^{M,N} = \frac{a_p^2}{8\mu\tau t_m} \Delta P_{net}^{M,N} \tag{19}$$

At the microscopic level, the non-steady state convective flux of the *solute* within the membrane pore  $(J_{i,filtration(solute)}^{pore})$  is modified due to the restriction caused by the solute-membrane interaction, and is given by the expression [69]:

$$\mathbf{J}_{i, filtration}^{pore} = \beta_i^{pore} C_i^{pore}(y) u_{pore}^{M,N} \tag{20}$$

Where  $\beta_i$  is the restriction coefficient and depends on the interactions between the solute and the porous wall, and  $C_i^{pore}(y)$  is the local concentration of the solute within the pore. The solute transport flux rate due to the hindered convection across the membrane from region M to N (also known as the solvent drag flux) is expressed as [70–73]:

Filtration – solute : 
$$J_{i,filtration}^{M,N} = \overline{C_i}^{M,N} (1 - \sigma_i) \quad u^{M,N}$$
 where; 
$$\overline{C_i}^{M,N} = \frac{C_i^M - C_i^N}{lnC_i^M - lnC_i^N}$$
 (21)

Where  $\overline{C_i}^{M,N}$  is the logarithmic mean average of the concentrations at the two sides of the membrane and  $(1-\sigma_i)$  represents the fraction of the solute dragged across the membrane by the fluid flow

# 4.2. Diffusion (Jdiffusion):

Diffusion transport flux moves substances passively from a higher concentration region to lower concentration. Similarly to convection, diffusion can be considered at two levels: (i) diffusion within the region (e.g., M), known as *free diffusion*, and (ii) diffusion across the membrane separating the regions (e.g., between M and N), which is known as *restricted diffusion*.

**(i) Diffusion-within the region (free diffusion):** The partial differential form of Fick's law below can be used to determine the free diffusive flux [74]:

$$\mathbf{J}_{i,diffusion}^{M} = -D_{i}^{M} \nabla C_{i}^{M} \tag{22}$$

Where  $D_i^M$  is the free diffusion coefficient for species 'i' in the control volume M, and has the unit  $(cm^2/s)$ . Depending on whether the molecule is charged or uncharged,  $D_i^M$  obtained using Eqs. (23), (24), and (25a), respectively.

The diffusion coefficient for an uncharged solute in a dilute liquid solution can be calculated either by applying the *Wilke – Chang* method (Eq. (23)) [45,75,76] or the *Stokes – Einstein* method (Eq. (24)) [49,67,77].

Wilke – chang: 
$$D_{i,uncharged}^{M} = 7.4 \times 10^{-15} \frac{T\sqrt{\varnothing_w M_w}}{(\sum \hat{v}_s)^{0.6} \mu}$$
 (23)

Stokes – Einstein: 
$$D_{i,uncharged}^{M} = \frac{K_B T}{6\pi a_s \mu}$$
 (24)

Where T is the temperature in Kelvin,  $\varnothing_W$  is the solvent association factor,  $M_W$  is the molecular weight of the solvent,  $\hat{v}_s$  is the molar volume of the solute, and  $\mu$  is the solvent viscosity,  $a_s$  is the radius of the spherical particle, and  $K_B$  is the Boltzmann's constant  $(1.38 \times 10^{-23} \ m^2 \cdot kg/(s^2 \cdot K))$ .

The free diffusion coefficient for a charged particle can be obtained from the expression [49]:

$$D_{i,charged}^{M} = \left(\frac{RT}{F^{2}}\right) \frac{\Lambda_{i}^{\infty}}{|z_{i}|}$$
 (25a)

Where R is the universal gas constant (8.314  $J/(mol \cdot K)$ ),  $z_i$  is the ionic charge, F is Faraday's constant (96, 490  $A \cdot s/mol$ ),  $\Lambda_i^{\infty}$  is the electrical conductance of ion 'i' in the solution ( $m^2/(ohm \cdot eq)$ ).

**(ii) Diffusion-through the membrane (restricted diffusion):** The one-dimensional restricted diffusion flux rate of a solute through a thin semipermeable membrane can be determined using Fick's equation as below:

$$J_{i,diffusion}^{pore} = -D_{i,eff}^{m} \frac{\partial C_{i}}{\partial V}$$
 (26)

Where  $D^m_{i,eff}$  is the *effective* diffusion coefficient of the solute in the membrane. The effective diffusion coefficient, also known as the restrictive diffusion coefficient, determines the effect of the heterogeneity and tortuosity of the biological membrane on the diffusion rate and is given by the expression [51,69,78]:

$$D_{i,eff}^{m} = \frac{\beta_i^m}{\tau^m} D_i^m \tag{27}$$

Where  $\beta_i^m$  and  $\tau^m$  are the solute restriction coefficient and tortuosity coefficient of the membrane layer, respectively.

The diffusive flux equation can be obtained in terms of the membrane permeability coefficient  $P_i^m$  (cm/sec) by integrating the

differential form of Fick's equation over the membrane thickness,  $t_m$  (cm)[47,79].:

$$J_{i,diffusion}^{M,N} = P_i^m \left( C_i^M - C_i^N \right) \tag{28}$$

Where  $J_{i,diffusion}^{M,N}$  has the unit of number of molecules per unit area per unit time. Permeability  $(P_i^m)$  is a phenomenological coefficient that relates the diffusion flux to the concentration gradient across the two sides of the membrane. The permeability of the porous membrane towards a molecule is usually determined experimentally; however, it can also be obtained theoretically using Eq. (29) [80].

$$P_i^m = \frac{K_i^m}{t_m} D_{i,eff}^m \tag{29}$$

Where  $K_i^m$  is the membrane partition coefficient for solute 'i'.

# 4.3. Migration (J<sub>migration</sub>):

The distribution of ions within a control volume or across the membrane can generate an electric field ( $\mathbf{E}$ , (V/m)). The produced electric field exerts an external force on charged particles, causing them to move either with or against the diffusive transport flux. This type of transport is known as *migration* and the migrative flux is obtained using the expression below [47,49,81,82]:

$$\mathbf{J}_{\mathbf{i},\mathbf{migration}}^{\mathbf{M}} = \mathbf{E} \nu_i^{M} \left( C_i^{M} \right) \tag{30}$$

Where  $v_i^M$ , and  $C_i^M$  are the electrokinetic mobility  $(m^2/(s \cdot V))$  and concentration of the ion, respectively. The single ion mobility  $(v_i^M)$  and the diffusion coefficient  $(D_i^M)$  are related by the expression:

$$\nu_i^M = \frac{D_i^M z_i F}{RT} \tag{31}$$

Where  $z_i$  is the valence of the ion, F is the Faraday's constant (96, 490  $A \cdot s/mol$ ), R is the universal gas constant (8.314  $J/(mol \cdot K)$ ) and T is the temperature in Kelvin.

The relationship between the electrical field (mV/cm) and the electric potential (mV) are given by:

$$\mathbf{E} = -\nabla \psi_E \tag{32a}$$

$$\nabla \psi_F^{M-N} = V_m^{M-N} = \psi^M - \psi^N \tag{32b}$$

Where  $\nabla \psi_E$  is the electrical potential gradient. The electrical potential gradient across the two sides of a thin membrane, which is known as the membrane voltage  $(V_m^{M,N})$ , can be obtained by using Eq. (32b).

# 5. Membrane mediated transport mechanisms:

After discussing the three main mass transport mechanisms, convection (filtration), diffusion, and migration, this section deals with transport across the membrane, which can be mediated via specific groups of integrated membrane proteins known as *transporters* [83]. Transporters are the class of membrane proteins including channels (ion channels and water channels), pumps, carrier-mediated proteins (uniporters, symporters, antiporters), and receptor-mediated transporters. These membrane proteins play a crucial role in maintaining the electrochemical gradient across the cell membrane, the uptake of nutrients, drug transport, and the removal of cell metabolism waste products [84,85]. For further details on the structure of these transporters, their molecular mechanisms, and their application in drug transport, please refer to references [26,86–94].

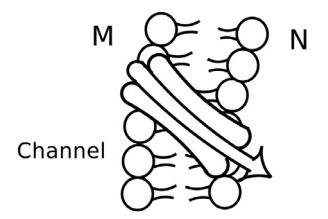


Fig. 5. Channel Transport Mechanism.

## 5.1. Channels (Jionchannel, Jwaterchannel):

The lipid bilayer membrane of the cell is impermeable to highly charged and hydrophilic molecules, such as ions and water molecules. However, the cell membrane contains solute-specific proteins known as channels that allow water molecules and charged substances to diffuse or migrate through them (see Fig. 5) [26,95]. Some of these channels are mainly permeable to ions, and are thus called ion channels, while those that are permeable to water molecules are known as water channels or aquaporins.

# 5.1.1. Ion channel (Jionchannel):

Ion channels create pathways for the passive movement of charged, hydrophilic molecules by diffusion and migration mechanisms. Various mathematical models can be used for the ion flux through ion channels. In order for these models to be precise, the size of the ion, possible reactions among the ions in the pathway, and interactions of the wall of the protein channel with the ion being transported should be considered [40,96–98]. Here, the ion channel models are classified depending on their scale as (i) ion distribution within (inside) the channel (ii) the net driven ion flux through the ion channels from one side (M) of the membrane containing the ion channels to the other (N).

**(i) Ion flux within (alongside) the channel:** The total ion flux within a channel is commonly modeled using a modified form of the Nernst-Planck equation. The Nernst-Planck equation gives the total ionic flux as the balance between the diffusive flux (Eq. (22)) and the electrical drift (Eq. (30)) and can be written as below [81,96,99]:

$$\mathbf{J_{i}^{ion}}^{channel} = -D_{i}^{m} \left( \nabla C_{i} + \left( \frac{z_{i}F}{RT} \right) C_{i} \nabla \psi_{i}^{eff} \right)$$
 (33)

Where  $D_i^m$  is the ion diffusion coefficient and can be obtained theoretically using Eq. (25a), and  $\nabla \psi_i^{eff}$  is the effective potential, which depends on the electrostatic potential and the interactions between transferring ions and the channel wall.

The one-dimensional volume-averaged ion flux over the cross-sectional area of the channel can be given as [49]:

$$\overline{\mathbf{J}_{i}^{\text{ion channel}}} = -D_{i,eff}^{m} \left( \frac{d\overline{C_{i}(y)}^{\text{ion channel}}}{dy} + \left( \frac{z_{i}F}{RT} \right) \overline{C_{i}}^{\text{ion channel}} \frac{d\psi_{i}^{\text{eff}}(y)}{dy} \right)$$
(34)

Where  $D_{ion,eff}^{m}$  is the restrictive diffusion coefficient for the ion and can be obtained by applying Eq. (25a) in Eq. (27).

The one-dimensional form of the Poisson equation (Eq. (35)) relates the spatial electric field distribution to the local charge density ( $\sigma(y)$ ) via the expression below [49]:

$$\sigma(y) = -\varepsilon_0 \frac{d^2 \psi^{eff}}{dy^2} = F \sum_{i=1}^m z_i \overline{C_i(y)}^{ion \ channel} + \sigma_p(y)$$
 (35)

Where  $\varepsilon_0$  is the dielectric constant (electrical permeability), the expression " $F\sum_{i=1}^m z_i \overline{C_i(y)}^{ion\ channel}$ ," sums the charge density on each of the 'm' individual ions, and  $\sigma_p(y)$  is the charge density on the immobilized protein wall of the membrane channel.

The combination of Eq. (34) with Eq. (35) is known as the Poisson-Nernst-Planck (PNP) model, and can be used develop a full model of ion distribution along the ion channels [96].

(ii) Net driven ion flux through the channel: The net ion flux from region M to N through the channel  $(mol/cm^2 \cdot s)$  is related to the current across the membrane  $(A/cm^2)$  by the expression[100]:

$$J_{i,ion\ channel}^{M,N} = \frac{I'r_{i,channel}^{M,N}}{z_i F}$$
 (36)

Where  $I''^{M,N}_{i,channel}$  is the net current density of ion 'i' through  $n_{i,channel}$  channels sensitive to ion 'i', and is given by the expression:

$$\begin{split} I''^{M,N}_{i,channel}(V_m,t) &= n''_{i,channel} \quad f^{i,channel}_o(V_m,t) \quad i^{M,N}_{i,channel}(V_m,t) \\ &= O^{channel}_i(V_m,t) \quad i^{M,N}_{i,channel}(V_m,t) \end{split} \tag{37}$$

Where  $n_{i,channel}''$  is the ion channel density per unit area of the membrane,  $f_o^{channel}(V_m,t)$  is the probability that the ion channel is in open state at time t and has a value between 0 and 1  $(0 \le f_o^{channel} \le 1)$ .

Most of these channels are not always open, and can be switched between at least two states (the open and closed states) in response to a chemical, electrophysiological, or hormonal stimulus. The probability that the channel will be open is a function of the membrane potential  $(V_m)$  and the channel structure; the product  $n''_{i,channel}f_o^{i,channel}$  is sometimes denoted by a single variable,  $O_i^{channel}$ , which refers to the total number of open channels per unit area of the membrane  $(A_m)$  (# of channels/cm²). Details of the types of gating are beyond the scope of this work. For further details, one can refer to references [87], [26], and [101–104].

 $i_i^{M,N}(V_m,t)$  is the current driven across the membrane through one channel (from region M to N). The ion current through the lipid bilayer membrane be modeled in two ways: using the Ohm model (Eq. (38)) or the Goldman-Hodgkin-Katz (GHK) model (Eq. (41)).

Ohm model: The current through a gating channel  $(i_{i,OhmChannel}^{M,N})$  according to Ohm's law is given by the expression below [102,105]:

$$i_{i,Ohm}^{M,N} = g_{i,channel}(V_m, C, t) \quad \left(V_m^{M,N} - V_{i,rev}^{M-N}\right)$$
(38)

Where  $g_{i,channel}$  ( $V_m$ , C, t) is the membrane conductance for channels of ion 'i' (channel conductance) in units of Siemens (S=1/Ohms) and can be a function of membrane voltage ( $V_m$ ), ion concentration (C) and time (t),  $V_m^{M,N}$  is the membrane voltage (Eq. (32b)), and  $V_{i,rev}^{M-N}$  is the membrane reversal potential for a single ion 'i'. At equilibrium, there is a balance between the electrical and chemical forces, and consequently, there is no net ionic flux across the membrane; otherwise, the membrane potential will vary and produce an electric field across the membrane, which in turn produces an ion flux across the membrane. The membrane potential, which is also known as the equilibrium or resting potential, at the equilibrium state (zero current) is known as the reversal potential, and can be calculated for a particular charged ion 'i' using the Nernst-potential equation below:

$$V_{i,rev}^{M-N} = -\frac{RT}{z_i F} ln \left( \frac{C_i^{M(in)}}{C_i^{N(out)}} \right)$$
(39)

The overall current flux (per unit area of the membrane) of the individual ion i' using the Ohm model is given below:

Ohm current model:

$$\begin{split} I'r_{i,Ohmchannel}^{M,N} &= n \nu_{i,channel} \quad f_o^{i,channel}(V_m,t) \quad g_{i,channel} \\ \left(V_m - V_{i,rev}^{M-N}\right) &= O_i^{channel}(V_m,t) \quad g_{i,channel} \quad \left(V_m - V_{i,rev}^{M-N}\right) \end{split} \tag{40}$$

Goldman-Hodgkin-Katz current model: If the ion channel is sufficiently short, and the charge density of the protein channel does not exceed the ion charge density, the right-hand side of the Poisson equation (Eq. (35)) becomes zero. These assumptions lead to a fixed electric potential and electric field across the membrane  $(d\psi/dy = -\psi^m/t_m)$ . The Goldman-Hodgkin-Katz (GHK) model approximates the ionic flux across the membrane through a given ion channel by assuming a constant electric field across the membrane. The GHK equation for outward ion current across the membrane from M to N is written as [106]:

$$i_{i,CHK}^{M,N} = P_i^{M-N} \frac{z_i^2 F^2 V_m^{M-N}}{RT} \frac{C_i^M - C_i^N exp \frac{-z_i F V_m^{M-N}}{RT}}{1 - exp \frac{-z_i F V_m^{M-N}}{RT}}$$
(41)

Where  $P_i^{M-N}$ , which has units of  $(cm/(pore \cdot s))$ , is the membrane permeability towards the specific ion 'i' through a single pore, and determines the amplitude of the membrane conductance for that ion.

The overall individual ionic current carried by ion 'i' per unit area of the membrane can be calculated using the GHK model as [102,107]:

$$I_{i,CHKChannel}^{\prime\prime M,N} = \tag{42}$$

$$nw_{i,channel} f_o^{i,channel} P_i^{M-N} \frac{z_i^2 F^2 V_m^{M-N}}{RT} \frac{C_i^M - C_i^N \exp{\frac{-z_i F V_m^{M-N}}{RT}}}{1 - \exp{\left(\frac{-z_i F V_m^{M-N}}{RT}\right)}} = (42)$$

$$O_{i}^{channel}P_{i}^{M-N}\frac{Z_{i}^{2}F^{2}V_{m}^{M-N}}{RT}\frac{C_{i}^{M}-C_{i}^{N}\exp\frac{-z_{i}FV_{m}^{M-N}}{RT}}{1-\exp\left(\frac{-z_{i}FV_{m}^{M-N}}{RT}\right)}$$
(42)

# 5.1.2. Water channel ( $J_{\text{waterchannel}}$ )

The small polar and uncharged molecule water can move across the cell membrane by the simple diffusion mechanism. However, the diffusion of water through the lipid membrane is relatively slow; therefore, additional pathways for the movement of water across the membrane must exist. Recent studies have shown that the cell membrane contains water channels, known as *Aquaporins* (AQP), that allow the passage of lipophobic water molecules through the cell membrane [83,108,109]. These channels play a crucial role in regulating the cell volume as well as in pathological conditions [110,111]. More details about the discovery and various types of water channels and their structure, regulation, and distribution in different cell and tissue types in the body can be found in references [112–115]. The water flux through the water channels can be expressed as [100,116–118]:

$$J_{waterchannel}^{M,N} = L_{water,p}^{AQP} \left( \Delta P_{hydraulic}^{M,N} - \sum_{i} \sigma_{i}^{MN} \Delta \pi_{i}^{M,N} - \sigma_{p} \Delta \prod_{p.oncotic}^{M,N} \right)$$
(43)

Where  $L_{water,p}^{AQP}$  is the hydraulic conductivity of the membrane towards water,  $\Delta P_{hydraulic}$  is the hydraulic pressure difference,  $\Delta \pi_{osmosis}$  is the osmotic pressure difference (Eq. (16b)), and  $\sigma_i$  is the reflection coefficient, which determines the real contribution of the osmotic pressure to the driven water flux through these channels.  $\Delta \prod_{p,oncotic}$  is the oncotic or colloid osmotic pressure difference, which corresponds to the osmotic pressure created by high-molecular-weight plasma proteins. The oncotic pressure difference can empirically be determined using the Landis and Pappenheimer model (Eq. (44)) [119–121]:

$$\prod\nolimits_{oncotic,total}^{M} = 2.1 \quad C_{protein}^{M} + 0.16 (C_{protein}^{M})^{2} + 0.009 (C_{protein}^{M})^{3} \quad (44)$$

Where  $\prod_{oncotic,total}^{M}$  is the plasma colloid osmotic pressure, and  $C_{protein}^{M}$  is the total plasma protein concentration within the region M (grams of protein per 100 liters of solution).

5.2. Carrier — mediated/transport ( $J_{uniporter}$ ,  $J_{pump}$ ,  $J_{symporter}$ ,  $J_{antiporter}$ ):

Some lipid-insoluble substances have low permeabilities across the cell membrane, or are too large to enter the cell via filtration and diffusion mechanisms or move through membrane channels and pores. Moreover, in some situations, a cell must import a solute against the direction of the electrochemical gradient to meet its needs. In these scenarios, the relevant solute may cross the membrane via membrane-integrated proteins known as carriers; the corresponding transport mechanism is known as carriermediated transport. Similarly to channels, these transporters are highly solute-specific; however, unlike channels, they do not contain hydrophobic pores. Therefore, carriers can only bind to one or a few substrate molecules at a time, and transport via carriers is much slower than via channels. Carrier-mediated transport is a multi-step process. Its underlying mechanism is briefly addressed below and schematically depicted in Fig. 6. In the first step, the substrate being transported (ligand) participates in a reversible binding (association) reaction with the binding site of the carrier on one side of the membrane (see Fig. 6 b and c). After the carrier-substrate complex has been formed, the carrier undergoes a conformational change and translocates the substrate across the membrane. Finally, the carrier releases the substrate at the other face through a dissociation reaction. Energy is needed to achieve the conformational change; depending on the source of the energy, the carrier is categorized as a uniporter, pump, symporter, and antiporter.

The uniport transport mechanism is a *passive* transport mechanism, as the carrier facilitates the downhill movement of a single group of specific large polar molecules across the membrane, such as glucose and amino acids, which cannot easily penetrate the membrane. For this reason, transport through uniporters is often referred to as "facilitated diffusion", in the sense that the membrane transporter facilitates the transport driven by the concentration gradient between the two regions (e.g., M and N) [122,123]. However, it differs from other passive transport mechanisms (diffusion, migration, convection, and channels) as the solute participates in a series of biochemical reactions with the fixed membrane carrier to cross the membrane [122,124,125].

Active transport mechanisms are typically used by cells to transport components against the electrochemical gradient. For this movement to take place, an additional source of energy is needed. This extra energy can be supplied by coupling the transport of the solute to another cellular reaction or transport phenomenon. Depending on the source of the supplied energy, the transport mechanism can be classified as *Primary active transport* or *Secondary active transport* [17,126,127].

In primary active transport, the cell directly utilizes chemical energy stored in chemical bonds, which is mainly released by the hydrolysis of adenosine triphosphate molecules or an equivalent high-energy phosphoryl bond. Adenosine triphosphate, which is abbreviated as ATP, is known as the energy molecule of the cell. ATP molecules can release a large amount of energy via their conversion to adenosine diphosphate (ADP) and the release of a phosphate ( $P_i$ ) ion group (ATP <=> ADP + $P_i$ ). ATPase is the enzyme that catalyzes the ATP dephosphorylation reaction. For this reason, this family of transporters is commonly known as "ATPase pumps" and/or "ATP powered pumps" [95,125,128].

Secondary active transport mechanisms couple the electrochemical potential produced across the membrane during the

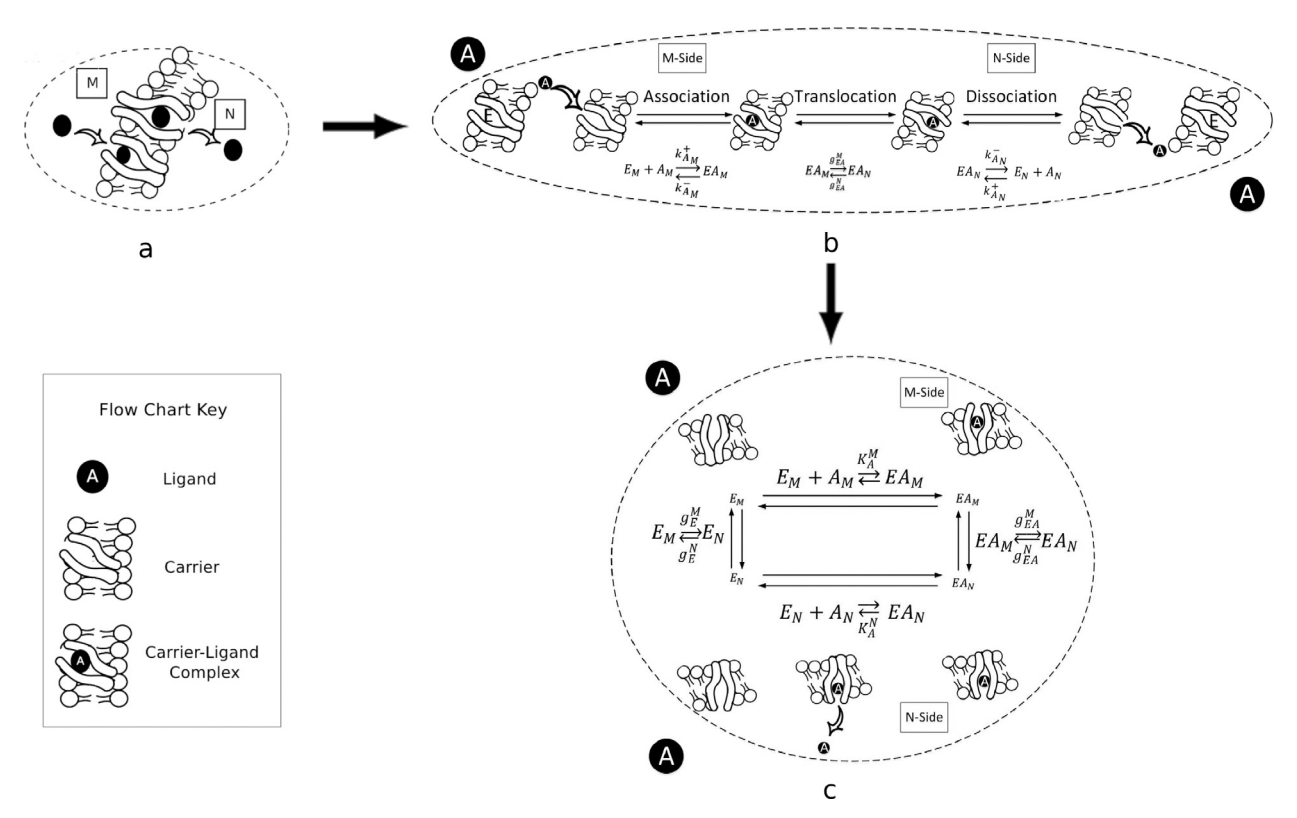


**Fig. 6.** A possible process by which a carrier protein can mediate the transport of a solute molecule across the lipid bilayer membrane. Figure a represents a uniporter (E), which transports a single solute (A) from one side of the membrane (M) to the other (N). Figures b and c represent the step-wise transport mechanism of solute (or ligand) A from one side of the membrane to the other side, besides the corresponding kinetic terms. First, the ligand binds the carrier on one side of the membrane (M) to form a  $EA_M$  complex; next, this complex passes the ligand across the membrane through a translocation step (carrier conformational shift) and then dissociates at the N side of the membrane. In Figure b,  $k_A^{+M}$  and  $k_A^{-M}$  are the association and dissociation rates, and superscripts show the side of the membrane that the reaction is taking place (sides M or N of the membrane).  $g_{EA}^M$  and  $g_{EA}^M$  are the carrier-ligand translocation rate constants with superscripts representing the side of the membrane translocation originates in (e.g.,  $g_{EA}^M$  is the translocation rate constant from M side to N side of the membrane). In Figure c,  $K_A^M$  is the dissociation equilibrium constants and is defined as  $K_A^M = k_A^{-M}/k_A^{N-M}$ . Moreover, in Figure c, there are two cycles: the inner cycle represents the forward substrate transport (influx); the outer cycle represents the backward flux (efflux).

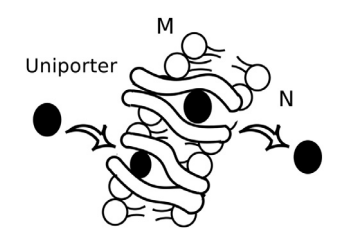


Fig. 7. Uniporter Transport Mechanism.

transport of one group of components to the simultaneous uphill transport of another group of substances [129,130]. The required electrochemical energy can be obtained from the simultaneous downhill transport of another family of solutes by the same transporter, or it can be exerted by the indirect involvement of the ATP hydrolysis reaction during the primary active transport of the other substrates. Cotransporters are capable of transporting two or more different families of solutes, and secondary active transporters can be further categorized as *symporters* and *antiporters*. The transport mechanism in which both types of solutes move in the same direction relative to each other is called symport transport, whereas the mechanism in which the solutes move in opposite directions is referred to as antiport transport.

The approach taken in developing the mathematical model of the transported flux driven via carriers differs from the ones discussed in earlier sections of this work. Since these transporters are embedded in the phospholipid bilayer membrane, they cannot dif-

fuse across the membrane. Therefore, in the mathematical equations related to the carrier transport mechanism, there is no term associated with the diffusion coefficient, and the thermal behavior of the molecules is captured in the reaction rate coefficients. Consequently, to develop a quantitative model of the flux transported by each transporter, one must know the rate expression of all steps, including the association and dissociation constants for the reaction steps occurring on the membrane surfaces, as well as the translocation rate constants for translocating the unloaded and loaded carriers. The rate constants for the binding and unbinding of solute A on the surface of the membrane can be determined experimentally, and are  $k_{A_M}^+$  and  $k_{A_M}^-$ , respectively for the M side; the equivalent values for the N side are  $k_{A_N}^+$  and  $k_{A_N}^-$  (Fig. 6b) [131]. The translocation rate of the transporter (denoted as  $g_E$ ,  $g_{EA}$ , etc.) determines the number of molecules that the transporter can transport per one molecule of the carrier. The translocation rate constants are a function of the membrane permeability (P) to the transporter in addition to the total available number of transporters ( $[E]_t$ ) and have units of inverse seconds (1/s) ( $g = P[E]_t$ ). The carrier translocation rate constants and the total amount of the carrier are experimentally determined.

The kinetic models for each individual carrier differ from one another with respect to some details of their mechanisms and the solute transported. For some of these transporters to translocate the solutes, the binding and unbinding of each of the solutes must occur in a particular order. Furthermore, in some cases, several substances (competitors) compete with the solutes being trans-

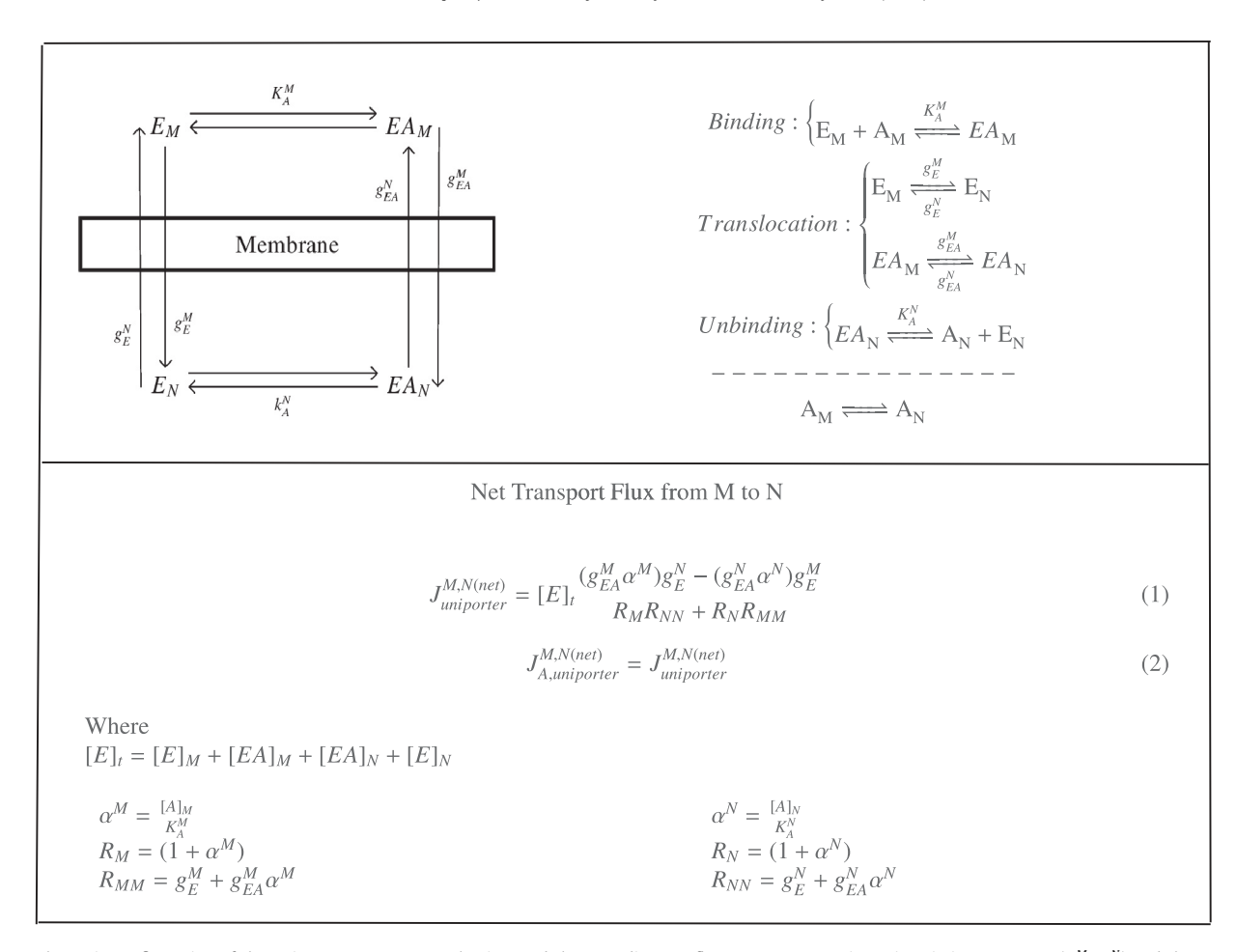


**Fig. 8.** A schematic configuration of the uniporter transport mechanism and the regarding net flux transport equation. Dissociation constants  $(K_A^M, K_A^N)$  and the translocation rate constants  $(g_E^M, g_E^M, g_E^M, g_E^M, g_E^N, g_E^M)$  are depicted in the reaction cycle in the right panel.  $[E]_I$  is the total number of transporter per unit area of the membrane. The flux equation is transformed to the general form of the resistance parameters from Stein model [131].

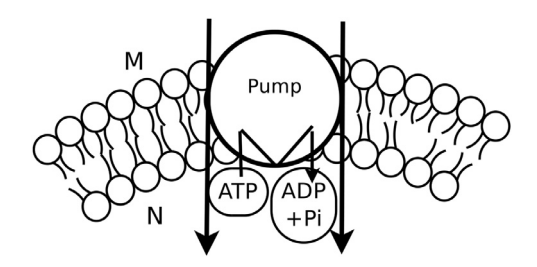


Fig. 9. ATPase Transport Mechanism.

ported during each translocation cycle for the same binding sites on the carrier. To reduce the modeling complexity of the transport mechanisms while still obtaining accurate prediction of the transported fluxes, one can make appropriate simplifying assumptions. The *rapid equilibrium* and *quasi-steady-state* assumptions are commonly used assumptions that are applied to most of the models discussed in this paper. Another assumption that is occasionally used is the *carrier symmetric assumption*. Each of these assumptions is discussed in more detail below. In the "rapid equilibrium assumption", the surface binding and unbinding reactions are assumed to occur much faster than the translocation of the complexes between the two sides of the membrane. That is, the rate-limiting step of the transport cycle is the translocation of the carrier-solute complexes from one side of the membrane to the

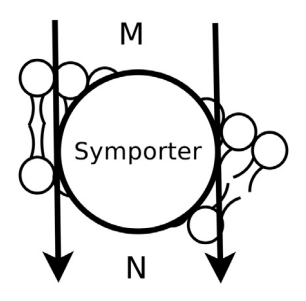


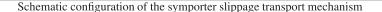
Fig. 10. Symporter Transport Mechanism.

other. The rapid equilibrium assumption allows the concentrations at the membrane surfaces to be determined by assuming that the equilibrium constant coefficients are independent of the reaction

path (e.g., in Fig. 6 b and c, 
$$K_A^M = \frac{k_{AM}^-}{k_{AM}^+} = \frac{[A]_M[E]_M}{[EA]_M}$$
 for side M, and

$$K_A^N = \frac{k_{A_N}^-}{k_{A_N}^+} = \frac{[A]_N[E]_N}{[EA]_N}$$
 for the other surface) [131].

In the "quasi-steady-state", it is assumed that due to the high affinity of the substrates with respect to the carrier, the concentration of the intermediate complex does not change on the time scale of carrier production rate, and the total number of carriers per unit area of the membrane ( $[E]_t$ ) is conserved during each cycle (i.e., in Fig. 6,  $[E]_t \ll [A] \Rightarrow \frac{d[EA]}{dt} = 0$ ).



$$E_{M} \xrightarrow{K_{B}^{M}} EB_{M}$$

$$E_{A} \xrightarrow{K_{AB}^{M}} EA_{M} \xrightarrow{K_{AB}^{M}} EAB_{M}$$

$$E_{A} \xrightarrow{g_{EA}^{M}} g_{EA}^{M} \xrightarrow{g_{EA}^{M}} EB_{N} \xrightarrow{g_{EAB}^{M}} g_{EAB}^{M}$$

$$EA_{N} \xrightarrow{EAB_{N}} EAB_{N}$$

$$Binding: \begin{cases} A_{M} + E_{M} & \stackrel{K_{A}^{M}}{\longleftrightarrow} EA_{M} \\ EA_{M} + B_{M} & \stackrel{K_{AB}^{M}}{\longleftrightarrow} EAB_{M} \\ B_{M} + E_{M} & \stackrel{K_{B}^{M}}{\longleftrightarrow} EB_{M} \\ EB_{M} + A_{M} & \stackrel{K_{BA}^{M}}{\longleftrightarrow} EAB_{M} \end{cases}$$

$$Translocation: \begin{cases} E_{M} \xrightarrow{g_{A}^{N}} E_{N} \\ EA_{M} \xrightarrow{g_{EA}^{M}} EA_{N} \\ EAB_{M} \xrightarrow{g_{EAB}^{M}} EAB_{N} \end{cases}$$

$$Unbinding: \begin{cases} \mathsf{EAB}_{N} \overset{\mathcal{K}_{AB}^{N}}{\Longleftrightarrow} \mathsf{B}_{N} + \mathsf{EA}_{N} \\ \mathsf{EAB}_{N} \overset{\mathcal{K}_{BA}^{N}}{\Longleftrightarrow} \mathsf{A}_{N} + \mathsf{EB}_{N} \\ \mathsf{EA}_{N} \overset{\mathcal{K}_{A}^{N}}{\Longleftrightarrow} \mathsf{A}_{N} + \mathsf{E}_{N} \\ \mathsf{EB}_{N} \overset{\mathcal{K}_{B}^{N}}{\Longleftrightarrow} \mathsf{B}_{N} + \mathsf{E}_{N} \\ \end{cases}$$

## Net Transport Flux from M to N

$$J_{A, symporter}^{M, N(net)} = \left[E_{I}\left(\frac{(g_{EA}^{M}\alpha^{M} + g_{EAB}^{M}\alpha^{\prime M}\beta^{M})(g_{E}^{N} + g_{EB}^{N}\beta^{N}) - (g_{EA}^{N}\alpha^{N} + g_{EAB}^{N}\alpha^{\prime N}\beta^{N})(g_{E}^{M} + g_{EB}^{M}\beta^{M})}{R_{M}R_{NN} + R_{N}R_{MM}}\right)\right]$$
(1a)

$$J_{B,symporter}^{M,N(net)} = \\ [E]_{t} \left( \frac{(g_{EB}^{M} \beta^{M} + g_{EAB}^{M} {\alpha'}^{M} \beta^{M})(g_{E}^{N} + g_{EA}^{N} {\alpha'}^{N}) - (g_{EB}^{N} \beta^{N} + g_{EAB}^{N} {\alpha'}^{N} \beta^{N})(g_{E}^{M} + g_{EA}^{M} {\alpha'}^{M})}{R_{M} R_{NN} + R_{N} R_{MM}} \right)$$
(1b)

Where

$$[E]_t = [E]_M + [EB]_M + [EA]_M + [EAB]_M + [EAB]_N + [EA]_N + [EB]_N + [E]_N$$

$$\alpha^{M} = \frac{[A]_{M}}{K_{A}^{M}}, \ \alpha'^{M} = \frac{[A]_{M}}{K_{B}^{M}}, \ \beta^{M} = \frac{[B]_{M}}{K_{B}^{M}}$$
 
$$\alpha^{N} = \frac{[A]_{N}}{K_{A}^{N}}, \ \alpha'^{N} = \frac{[A]_{N}}{K_{B}^{N}}, \ \beta^{N} = \frac{[B]_{N}}{K_{B}^{N}}$$
 
$$R_{M} = (1 + \alpha^{M} + \beta^{M} + \alpha'^{M}\beta^{M})$$
 
$$R_{MM} = g_{E}^{M} + g_{EA}^{M}\alpha^{M} + g_{EB}^{M}\beta^{M} + g_{EAB}^{M}\alpha'^{M}\beta^{M}$$
 
$$R_{NN} = g_{E}^{N} + g_{EA}^{N}\alpha^{N} + g_{EB}^{N}\beta^{N} + g_{EAB}^{N}\alpha'^{N}\beta^{N}$$
 
$$R_{NN} = g_{E}^{N} + g_{EA}^{N}\alpha^{N} + g_{EB}^{N}\beta^{N} + g_{EAB}^{N}\alpha'^{N}\beta^{N}$$

**Fig. 11.** (a) A schematic configuration of the symport slippage transport mechanism and the regarding net transport flux. Dissociation constants  $(R_A^M, K_{BA}^M, K_{BA}^M)$  and the translocation rate constants  $(g_E^M, g_{EA}^M, g_{EA}^M, g_{EA}^M)$  are depicted in the reaction cycle in the left panel.  $[E]_t$  is the total number of transporter per unit area of the membrane. In this model empty carrier and the partially loaded carrier can slipp across the membrane. The flux equation is transformed to the general form of the resistance from Stein model [131] (part 1/2 continued on the next page). (b) A schematic configuration of the symport slippage transport mechanism and the regarding net flux transport equation. Dissociation constants  $(K_A^M, K_{BA}^M, K_B^M)$  and the translocation rate constants  $(g_E^M, g_{EA}^M, g_{EB}^M, g_{EB}^M, g_{EB}^M, g_{EB}^M)$  are depicted in the reaction cycle in the left panel.  $[E]_t$  is the total number of transporter per unit area of the membrane. In this model empty carrier and the partially loaded carrier can slipp across the membrane. The flux equation is transformed to the general form of the resistance from Stein model [131] (part 2/2 continued from previous page).

Schematic configuration of the two-substrate symporter ordered binding transport mechanism, where A binds first 
$$\begin{cases} A_{M} + E_{M} \xrightarrow{K_{A}^{N}} EA_{M} \mid EA_{M} + B_{M} \xrightarrow{K_{AB}^{N}} EAB_{M} \\ A_{M} + E_{M} \xrightarrow{K_{AB}^{N}} EA_{M} \mid EA_{M} + B_{M} \xrightarrow{K_{AB}^{N}} EAB_{M} \end{cases}$$

$$E_{M} \xrightarrow{K_{AB}^{N}} EA_{M} \xrightarrow{K_{AB}^{N}} EAB_{M} \qquad \begin{cases} E_{M} \xrightarrow{K_{AB}^{N}} EA_{M} + B_{M} \xrightarrow{K_{AB}^{N}} EAB_{M} \\ EAB_{M} \xrightarrow{K_{AB}^{N}} EAB_{M} & EAB_{M} \end{cases}$$

$$EAB_{M} \xrightarrow{K_{AB}^{N}} EAB_{M} \qquad \begin{cases} EAB_{M} \xrightarrow{K_{AB}^{N}} EAB_{M} & EAB_{M} \\ EAB_{M} \xrightarrow{K_{AB}^{N}} EAB_{M} & EAB_{M} \end{cases}$$

$$EAB_{M} \xrightarrow{K_{AB}^{N}} EAB_{M} + B_{M} \mid EAA_{M} + B_{M} \Rightarrow A_{M} \Rightarrow A_{M} + B_{M} \Rightarrow A_{M} \Rightarrow A_{$$

**Fig. 12.** A schematic configuration and the regarding net flux transport equation of the symporter ordered binding with no slippage, for transport of two solutes where A binds first. Dissociation constants ( $K_A$  and  $K_{AB}$  terms) and the translocation rate constants ( $K_B$  and  $K_{AB}$  terms) are depicted in the reaction cycle in the left panel. [E]<sub>t</sub> is the total number of transporter per unit area of the membrane. The flux equation is transformed to the general form of the resistance from Stein model [131].

In the "carrier symmetry assumption," the dissociation constants on both sides of the membrane are the same (e.g.,  $K_A^M = K_A = K_A$  in Fig. 6-c) and that the backward and forward translocation reactions of the carrier occur at the same speed (e.g., in Fig. 6,  $g_{EA}^M = g_{EA}^N = g_{EA}$  and  $g_E^M = g_E^N = g_E$ ). In the remainder of this work, detailed studies of each carrier

In the remainder of this work, detailed studies of each carrier group and several well-known kinetic models are presented. Furthermore, for each carrier, a simplified model and its simplifying assumptions are outlined. Subsequently, following the kinetic parameterization of Stein (2012) [131], all models are transformed into a general identical resistance parametric form. Each model includes a figure that demonstrates a possible kinetic model in the left panel, while the right panel depicts a related sequence of reaction equations that address the transport mechanism by the carrier (e.g., see Fig. 8). In each scheme, there are two cycles: the inner cycle represents the forward transport of substrates (influx); the outer cycle represents backward flux (efflux). The corresponding net flux of the carriers driven across the membrane is expressed as  $J_{carrier}^{M,N(net)} = J_{carrier}^{M,N} - J_{carrier}^{N,M}$ 

# 5.2.1. Uniporter Mmechanism ( $J_{Uniporter}$ ):

The uniport transport mechanism facilitates the downhill movement of a single group of specific large polar molecules across the membrane which cannot easily penetrate the membrane (see Fig. 7). Fig. 8 shows a possible reaction cycle for a uniporter (E) that can face the M side of the membrane, where it binds to solute A to form the complex  $EA_M$ . Next, the carrier-substrate complex translocates across the membrane with a translocation rate constant  $g_{FA}^{M}$ to face the other side of the membrane  $(EA_N)$ . In the last step, the loaded carrier  $(EA_N)$  undergoes a dissociation reaction that releases substrate A at the N side of the membrane. The translocation of the free carrier,  $E_M$  and  $E_N$ , takes place with translocation rate constants of  $g_E^M$  and  $g_E^N$ , respectively. Stein (2012) [131] developed this model using the following assumptions: 1) the binding and unbinding reactions of the solute are rapid relative to the translocation step, 2) the quasi-steady-state assumption is valid, and 3) the carrier is non-symmetric; therefore, distinct equilibrium constants  $(K_A^M$  and  $K_A^N)$  and different translocation constants  $(g_E^M, g_{EA}^M, g_E^N, g_{EA}^N)$  are considered. The net turnover rate of the uniporter and the flux of molecules of A transported through the uniporter from

$$J_{symporter}^{M,N(net)} = [E]_t \frac{G_{EAB} + J_{SE} - G_{EAB} + J_{SE}}{R_M R_{NN} + R_N R_{MM}}$$

$$J_{A,symporter}^{M,N(net)} = J_{symporter}^{M,N(net)}$$
(1b)

$$J_{R \ symporter}^{M,N(net)} = J_{symporter}^{M,N(net)} \tag{1c}$$

$$\begin{split} [E]_{t} &= [E]_{M} + [EB]_{M} + [EAB]_{M} + [EAB]_{N} + [EB]_{N} + [E]_{N} \\ \alpha'^{M} &= \frac{[A]_{M}}{K_{BA}^{M}}, \quad \beta^{M} &= \frac{[B]_{M}}{K_{B}^{M}} \\ R_{M} &= (1 + \beta^{M} + \alpha'^{M}\beta^{M}) \\ R_{MM} &= g_{E}^{M} + g_{EAB}^{M}\alpha'^{M}\beta^{M} \\ \end{split}$$

$$R_{NN} &= g_{E}^{N} + g_{EAB}^{N}\alpha'^{N}\beta^{N}$$

$$R_{NN} &= g_{E}^{N} + g_{EAB}^{N}\alpha'^{N}\beta^{N}$$

Fig. 13. A schematic configuration and the regarding net flux transport equation of the symporter mechanism with no slippage, for transport of two solutes where binding happens in order and B binds first. Dissociation constants ( $K_{BA}$  and  $K_{B}$  terms) and the translocation rate constants ( $g_{E}$  and  $g_{EAB}$  terms) are depicted in the reaction cycle in the right panel. [E]t is the total number of transporter per unit area of the membrane. The flux equation is transformed to the general resistance form from Stein model [131].

side M to side N of the membrane can be obtained using equations 45 and 46, respectively.

# Uniporter simplified model:

If one invokes the symmetric assumption for the dissociation constants (i.e.,  $K = K_A^M = K_A^N$ ), three different cases can be considered depending on the relative value of the translocation rate constant of the free carrier constant to that of the carrier-ligand complex  $(g_E$  to  $g_{EA})$  in addition to the solute concentration at the N side  $([A]_N)$  relative to the dissociation constant (K). The "one-way" solute flux for each case is expressed as below [49]:

case # 1)  $g_{EA} \gg g_E$  and  $[A]_N \geqslant K$ : In this situation, an increase in  $[A]_N$  leads to a higher transporter flux  $(J_{uniporter}^{M.N})$ :

$$J_{uniporter}^{M,N} = [E]_t g_{EA} \frac{[A]_M}{[A]_M (2 + \frac{K}{[A]_N}) + K}$$
(47)

case # 2)  $g_{EA} \ll g_E$  and  $[A]_N \leqslant K$ : In this situation, increases in  $[A]_N$  cause the transporter flux  $(J_{uniporter}^{M.N})$  from M to N to fall, and vice versa:

$$J_{uniporter}^{M,N} = [E]_t g_{EA} \frac{[A]_M}{[A]_M (1 + \frac{[A]_N}{[A]_{tr}}) + 2K}$$
(48)

case # 3)  $g_{EA} = g_E$ : The turnover of the loaded and unloaded carriers occurs at the same rate. In this case, when the concentration of the substrate is much higher than the availability of the carrier, the one-way flux of the solute from the M membrane surface to the N side will be:

$$J_{uniporter}^{M,N} = \left(\frac{[E]_t g_{EA}}{2}\right) \frac{[A]_M}{K + [A]_M}$$
(49)

Eq. (49) is identical to the single-substrate enzymatic Michaelis-Menten reactions on the surface of the membrane and describes the rate of uptake of the substance as:

$$J_{uniporter}^{M,N} = V_{\text{max}} \frac{[A]_M}{K_m + [A]_M}$$

$$\tag{50}$$

Where  $V_{\text{max}}$  and  $K_m$  are the Michaelis-Menten parameters. The maximum velocity  $(V_{max})$  occurs when the solute concentration reaches infinity starting from an initial value of zero, and corresponds to the number of available sites on the carrier for substance uptake. Comparing Eqs. (49) and (50), the maximum velocity of the reaction is  $V_{\text{max}} = \frac{[E]_t g_{EA}}{2}$ .  $K_m = K$  is the half-saturation rate constant and represents the concentration of the substrate at

Schematic configuration of the ABAC symporter transport mechanism, where the order of binding is A, B, second A, and C and the unbinding reactions occur in the reverse order of binding 
$$E_{M} \overset{K_{A}^{N}}{\longleftrightarrow} EA_{M} \overset{K_{AB}^{N}}{\longleftrightarrow} EAB_{M} \overset{K_{ABA}^{N}}{\longleftrightarrow} EABA_{M} \overset{K_{ABA}^{N}}{\longleftrightarrow} EABAC_{M}$$

$$E_{M} \overset{K_{A}^{N}}{\longleftrightarrow} EA_{N} \overset{K_{AB}^{N}}{\longleftrightarrow} EAB_{M} \overset{K_{ABA}^{N}}{\longleftrightarrow} EABAC_{M} \overset{K_{ABA}^{N}}$$

**Fig. 14.** (a) A schematic configuration of the ABAC symporter mechanism transporting of three solutes and the regarding net flux transport equation. In this configuration, the carrier exists in 5 different states on each side of the membrane. Dissociation constants ( $K_A$ ,  $K_{AB}$ ,  $K_{ABA}$ , and  $K_{ABAC}$  terms) and the translocation rate constants ( $g_E$ ,  $g_{EA}$ ,  $g_{EABA}$ , and  $g_{EABAC}$  terms) are depicted in the reaction cycle in the right panel. [E]<sub>t</sub> is the total number of transporter per unit area of the membrane. Transport equations are reparametrized and transformed into the general resistance form from Delpire model [134] (part 1/2 continued on next page). (b) A schematic configuration of the ABAC symporter mechanism transporting of three solutes and the regarding net flux transport equation. In this configuration, the carrier exists in 5 different states on each side of the membrane. Dissociation constants ( $K_A$ ,  $K_{AB}$ ,  $K_{ABA}$ , and  $K_{ABAC}$  terms) and the translocation rate constants ( $K_A$ ,  $K_{ABA}$ ,  $K_{ABA}$ , and  $K_{ABAC}$  terms) and the translocation rate constants ( $K_A$ ,  $K_{ABA}$ ,  $K_{ABAC}$  terms) are depicted in the reaction cycle in the right panel. [E]<sub>t</sub> is the total number of transporter per unit area of the membrane. Transport equations are reparametrized and transformed into the general resistance form from Delpire model [134] (part 2/2 continued from previous page).

which the half-maximal rate is observed. The half-saturation rate constant also determines the number of carrier turnovers and, consequently, the number of molecules of the solute transported by the carrier per unit time by each translocation of the solute-carrier complex.

# 5.2.2. Primary active transport mechanism (Jpump):

ATPase pumps use the energy released during ATP hydrolysis to pump one or more groups of ions and molecules against an uphill electrochemical gradient (see Fig. 9). The net result of the stepwise uphill transport of one substance (A) via an ATPase pump is summarized in the following reaction equation:

$$A_N + (ATP)_N \rightleftharpoons A_M + (ADP)_N + (Pi)_N$$

As is clear from the above reaction equation, the direction of transport depends on the concentration of ATP and ADP molecules in contact with the cell membrane, as well as the substrate concentrations ( $[A]_M$  and  $[A]_N$ ). ATP molecules are abundantly produced in the cell; therefore, normally the intracellular (N side) concentration of ATP is high, which results in a positive transport flux and allows the pump to pump A out of the cell (from N to M). This is advantageous when the pump is used to exclude A from the cell. If the concentration of  $A_M$  outside the cell is very high, the pump will work in the opposite direction, and A molecules will move from outside (M) to the inside (N) of the cell while contributing to ATP production [49].

For the primary active transport mechanism, the carrier can be present in three states: the empty unloaded carrier (E), the carrier-solute complex (EA), and the carrier-solute-phosphate bound complex (EAP). Among these three states, only the unloaded carrier (E) and the phosphorylated carrier-solute complex (EAP) can cross the

# Net Transport Flux from M to N

$$J_{A,symporter}^{M,N(net)} = [E]_{t}$$

$$\left(\frac{R_{NN}\left(g_{EA}^{M}\alpha^{M} + g_{EAB}^{M}\alpha^{M}\beta^{M} + g_{EABA}^{M}\alpha^{M}\beta^{M}\alpha^{\prime\prime M} + g_{EABAC}^{M}\alpha^{M}\beta^{M}\alpha^{\prime\prime M}\gamma^{M}\right)}{R_{M}R_{NN} + R_{N}R_{MM}}$$

$$-\frac{R_{MM}\left(g_{EA}^{N}\alpha^{N} + g_{EAB}^{N}\alpha^{N}\beta^{N} + g_{EABA}^{N}\alpha^{N}\beta^{N}\alpha^{\prime\prime N} + g_{EABAC}^{N}\alpha^{N}\beta^{N}\alpha^{\prime\prime N}\gamma^{N}\right)}{R_{M}R_{NN} + R_{N}R_{MM}}\right)$$

$$\left(1a\right)$$

$$J_{B,symporter}^{M,N(net)} = [E]_{t}$$

$$\left(\frac{R_{NN}\left(g_{EAB}^{M}\alpha^{M}\beta^{M} + g_{EABA}^{M}\alpha^{M}\beta^{M}\alpha^{\prime\prime M} + g_{EABAC}^{M}\alpha^{M}\beta^{M}\alpha^{\prime\prime M}\gamma^{M}\right)}{R_{M}R_{NN} + R_{N}R_{MM}}\right)$$

$$-\frac{R_{MM}\left(g_{EAB}^{N}\alpha^{N}\beta^{N} + g_{EABA}^{N}\alpha^{N}\beta^{N}\alpha^{\prime\prime N} + g_{EABAC}^{N}\alpha^{N}\beta^{N}\alpha^{\prime\prime N}\gamma^{N}\right)}{R_{M}R_{NN} + R_{N}R_{MM}}\right)$$
(1b)

$$J_{C,symporter}^{M,N(net)} = [E]_t \left( \frac{R_{NN}(g_{EABAC}^M \alpha^M \beta^M \alpha^{\prime\prime M} \gamma^M) - R_{MM}(g_{EABAC}^N \alpha^N \beta^N \alpha^{\prime\prime N} \gamma^N)}{R_M R_{NN} + R_N R_{MM}} \right)$$
(1c)

where

$$[E]_t = [E]_M + [EA]_M + [EAB]_M + [EABA]_M + [EABAC]_M + [EABAC]_N + [EABA]_N + [EAB]_N + [EA]_N + [EA]_N + [EA]_M + [EABA]_M + [EABA]_M + [EABAC]_M + [EABAC]_M + [EABAC]_M + [EABAC]_M + [EABA]_M + [EABAC]_M + [EABAC]_M$$

$$\alpha^{M} = \frac{[A]_{M}}{K^{M}}, \beta^{M} = \frac{[B]_{M}}{K^{M}}, \alpha^{\prime\prime\prime M} = \frac{[A]_{M}}{K^{M}}, \gamma^{M} = \frac{[C]_{M}}{K^{M}}$$

$$\alpha^{N} = \frac{[A]_{N}^{A}}{K^{N}}, \beta^{N} = \frac{[B]_{N}^{AB}}{K^{N}}, \alpha^{\prime\prime\prime N} = \frac{[A]_{N}}{K^{N}}, \gamma^{N} = \frac{[C]_{N}}{K^{N}}$$

$$R_{M} = 1 + \alpha^{M} + \alpha^{M}\beta^{M} + \alpha^{M}\beta^{M}\alpha^{\prime\prime\prime M} + \alpha^{M}\beta^{M}\alpha^{\prime\prime\prime M}\gamma^{M}$$

$$R_{N} = 1 + \alpha^{N} + \alpha^{N}\beta^{N} + \alpha^{N}\beta^{N}\alpha^{\prime\prime N} + \alpha^{N}\beta^{N}\alpha^{\prime\prime\prime N}\gamma^{N}$$

$$R_{MM} = g_{E}^{M} + g_{EA}^{M}\alpha^{M} + g_{EAB}^{M}\alpha^{M}\beta^{M} + g_{EABA}^{M}\alpha^{M}\beta^{M}\alpha^{\prime\prime\prime M} + g_{EABAC}^{M}\alpha^{M}\beta^{M}\alpha^{\prime\prime\prime M}\gamma^{M}$$

$$R_{NN} = g_{E}^{N} + g_{EA}^{N}\alpha^{N} + g_{EAB}^{N}\alpha^{N}\beta^{N} + g_{EABA}^{N}\alpha^{N}\beta^{N}\alpha^{\prime\prime\prime N} + g_{EABAC}^{N}\alpha^{N}\beta^{N}\alpha^{\prime\prime\prime N}\gamma^{N}$$

Fig. 14. Continued

membrane. Upon applying symmetric assumption for the translocation rate constants of the loaded and unloaded carriers ( $g_{EAP} = g_{EAP}^M = g_{EAP}^N$ ,  $g_E = g_E^M = g_E^N$ , and  $g_{EAP} = g_E = g$ ) and the symmetric dissociation constants between carrier and substance on both sides of the membrane ( $K_A = K_A^M = K_A^N$ ), the net flux driven across the membrane ( $J_{A,pump} = J_{A,pump}^{N,M} - J_{A,pump}^{M,N}$ ) is obtained from the expression [49]:

$$J_{A,pump} = [E]_{t}g\left(\frac{K_{A}(K_{EAP}^{M}[A]_{M} - K_{EAP}^{N}[A]_{N})}{(K_{EAP}^{M} + K_{EAP}^{M} + 2K_{EAP}^{M}K_{EAP}^{N})[A]_{M}[A]_{N}} - \frac{1}{+K_{A}(1 + 2K_{EAP}^{M})[A]_{M} + K_{A}(1 + 2K_{EAP}^{N})[A]_{N} + 2K_{A}^{2}}\right)$$
(51)

Where  $K_A = \frac{[A]_N [E]_N}{[EA]_N} = \frac{[A]_M [E]_M}{[EA]_M}$ ,  $K_{EAP}^N = \frac{[EAP]_N}{[EA]_N}$ , and  $K_{EAP}^M = \frac{[EAP]_M}{[EA]_M}$ .

# Pumps simplified model:

Another method to describe the flux of ion-coupled transport across the plasma membrane by an ATPase pump is to apply the Hill model (Eq. (9)). The Hill model of the ATPase pump is given by the expression [55,132]:

$$J_{A,pump} = J_{A,pump}^{\max} \left( \frac{[A]_N^{\eta_{pump}}}{[A]_N^{\eta_{pump}} + K_{pump}^{\eta_{pump}}} \right)$$
 (52)

Where  $J_{A,pump}^{\max}$  is the maximum velocity of uptake,  $\eta_{pump}$  is the Hill coefficient, and  $K_{pump}$  is the  $[A]_N$  concentration at which  $J_{A,pump}$  is half  $J_{A,pump}^{\max}$ . When  $\eta_{pump}=1$  this single-subtrate trans-

port model becomes similar to the Michaelis-Menten equation, and can be written as:

$$J_{A,pump} = J_{A,pump}^{max} \left( \frac{[A]_N}{[A]_N + K_{m,pump}} \right)$$
(53)

The primary active transport mechanism can also transport more than one substrate. Assuming that the ATPase pump actively transports a molecules of A from the M side of the membrane to its N side and simultaneously transports b molecules of B in the opposite direction (from N to M) with the corresponding ratio aA: bB, and further assuming the binding of each of the components to the carrier is an independent process, the overall transport reaction mechanism can be represented as

$$ATP + aA_M + bB_N \rightleftharpoons ADP + Pi + aA_N + bB_M$$

and the associated net fluxes of solutes A and B transported across the pump can be obtained using Eqs. (54a) and (54b), respectively, where the minus sign takes into account the direction of the flux of B [133]

$$J_{A,pump} = J_{A,pump}^{\text{max}} \left[ \frac{[A]_N}{[A]_N + K_A^N} \right]^a \left[ \frac{[B]_M}{[B]_M + K_B^M} \right]^b$$
 (54a)

$$J_{B,pump} = \frac{-b}{a} J_{A,pump}^{M,N} \tag{54b}$$

In Eq. (54a),  $J_{A,pump}^{\text{max}}$  is the maximum A efflux,  $K_A^M$ , and  $K_B^N$  are the apparent dissociation constants of the complexes created at the M or N sides of the membrane, respectively.

Schematic configuration of the ABCB symporter first on- first off transport mechanism, where order of binding is A,B,C, and second B and the order of unbinding is A, B, C, and B

$$E_{M} \overset{K_{A}^{M}}{\rightleftharpoons} EA_{M} \overset{K_{AB}^{M}}{\rightleftharpoons} EAB_{M} \overset{K_{ABC}^{M}}{\rightleftharpoons} EABC_{M} \overset{K_{ABCB}^{M}}{\rightleftharpoons} EABCB_{M}$$

$$g_{E}^{N} \overset{K_{ABCB}^{M}}{\rightleftharpoons} EB_{N} \overset{K_{ABCB}^{M}}{\rightleftharpoons} ECB_{N} \overset{K_{ABCB}^{M}}{\rightleftharpoons} EBCB_{N} \overset{K_{ABCB}^{M}}{\rightleftharpoons} EABCB_{N}$$

$$\begin{cases} A_{M} + E_{M} \overset{K_{ABC}^{M}}{\rightleftharpoons} EA_{M} \mid EA_{M} + B_{M} \overset{K_{ABC}^{M}}{\rightleftharpoons} EABCB_{N} \\ EAB_{M} + C_{M} \overset{K_{ABC}^{M}}{\rightleftharpoons} EABC_{M} \mid EABC_{M} + B_{M} \overset{K_{ABCB}^{M}}{\rightleftharpoons} EABCB_{M} \\ EABCB_{M} \overset{g_{EABCB}^{M}}{\rightleftharpoons} EBCB_{N} & EABCB_{N} \\ EABCB_{N} \overset{g_{EABCB}^{M}}{\rightleftharpoons} EABCB_{N} & EABCB_{N} \\ EABCB_{N} \overset{K_{ABCB}^{N}}{\rightleftharpoons} EBCB_{N} + A_{N} \mid EBCB_{N} \overset{K_{BCB}^{N}}{\rightleftharpoons} ECB_{N} + B_{N} \\ ECB_{N} \overset{K_{CB}^{N}}{\rightleftharpoons} EB_{N} + C_{N} \mid EB_{N} \overset{K_{B}^{N}}{\rightleftharpoons} E_{N} + B_{N} \end{cases}$$

Net Transport Flux from M to N

 $A_M + B_M + C_M \rightleftharpoons A_N + B_N + C_N$ 

$$J_{symporter}^{M,N(net)} = [E]_t \left( \frac{\left( g_{EABCB}^M \alpha^M \beta^M \gamma^M \beta^{\prime\prime M} \right) g_E^N - \left( g_{EABCB}^N \alpha^N \beta^N \gamma^N \beta^{\prime\prime N} \right) g_E^M}{R_M R_{NN} + R_N R_{MM}} \right)$$
(1a)

$$J_{A,symporter}^{M,N(net)} = J_{symporter}^{M,N(net)}$$
(1b)

$$J_{B,symporter}^{M,N(net)} = 2J_{symporter}^{M,N(net)}$$
(1c)

$$J_{C,symporter}^{M,N(net)} = J_{symporter}^{M,N(net)}$$
(1d)

where

$$[E]_t = [E]_M + [EAB]_M + [EABC]_M + [EABCB]_M + [EABCB]_N + [EABC]_N + [EABC]_N + [EAB]_N + [$$

$$\alpha^{M} = \frac{[A]_{M}}{K^{M}}, \quad \beta^{M} = \frac{[B]_{M}}{K^{M}_{N}},$$

$$\alpha^{N} = \frac{[A]_{N}}{K^{N}_{ABCB}}, \quad \beta^{N} = \frac{[B]_{N}}{K^{N}_{BCB}}$$

$$\gamma^{N} = \frac{[C]_{N}}{K^{N}_{ABCB}}, \quad \beta^{N'N} = \frac{[B]_{N}}{K^{N}_{B}},$$

$$\gamma^{N} = \frac{[C]_{N}}{K^{N}_{CB}}, \quad \beta^{N'N} = \frac{[B]_{N}}{K^{N}_{B}}$$

$$\begin{split} R_{M} &= 1 + \alpha^{M} + \alpha^{M}\beta^{M} + \alpha^{M}\beta^{M}\gamma^{M} + \alpha^{M}\beta^{M}\gamma^{M}\beta^{\prime\prime\prime M} \\ R_{N} &= 1 + \beta^{\prime\prime\prime N} + \gamma^{N}\beta^{\prime\prime N} + \beta^{N}\gamma^{N}\beta^{\prime\prime\prime N} + \alpha^{N}\beta^{N}\gamma^{N}\beta^{\prime\prime\prime N} \\ R_{MM} &= g_{E}^{M} + g_{EABCB}^{M}\alpha^{M}\beta^{M}\gamma^{M}\beta^{\prime\prime\prime M} \\ R_{NN} &= g_{E}^{N} + g_{EABCB}^{N}\alpha^{N}\beta^{N}\gamma^{N}\beta^{\prime\prime\prime N} \end{split}$$

**Fig. 15.** (a) A schematic configuration of the symporter mechanism transporting three solutes (ABCB), and the corresponding net transported flux equation. In this configuration, the carrier exists in 5 different states on each side of the membrane. Dissociation constants ( $K_A$ ,  $K_{AB}$ ,  $K_{ABC}$ ,  $K_{ABCB}$ ,  $K_{CB}$ , and  $K_B$  terms), and the translocation rate constants ( $g_E$  and  $g_{EABCB}$  terms) are depicted in the reaction cycle in the right panel. [E] $_t$  is the total number of transporter per unit area of the membrane (part 1/2 continued on next page). (b) A schematic configuration of the symporter mechanism transporting three solutes (ABCB), and the corresponding net transported flux equation. In this configuration, the carrier (cotransporter) exists in 5 different states on each side of the membrane. Dissociation constants ( $K_A$ ,  $K_{AB}$ ,  $K_{ABC}$ ,  $K_{ABCB}$ ,  $K_{CB}$ , and  $K_B$  terms), and the translocation rate constants ( $g_E$  and  $g_{EABCB}$  terms) are depicted in the reaction cycle in the right panel. [E] $_t$  is the total number of transporter per unit area of the membrane (part 2/2 continued from last page).

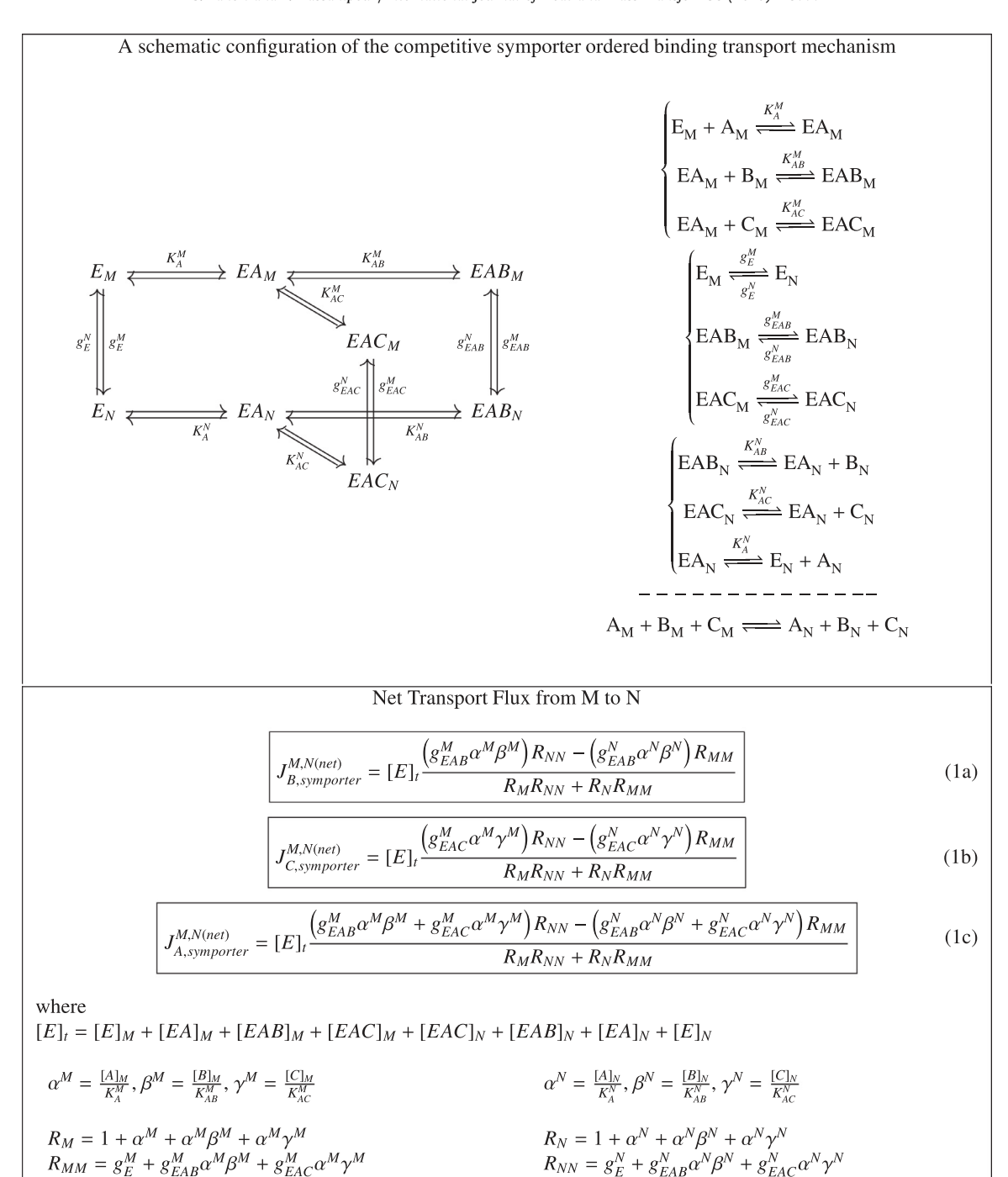


**Fig. 16.** (a) A schematic configuration of the competitive symporter ordered binding transport mechanism of two solutes and the regarding net flux transport equation. In this configuration, the carrier exists in four different states on each surface of the membrane. Transport equations are reparametrized and transformed into the general resistance form from Layton model [100]. Dissociation constants ( $K_A$ ,  $K_{AB}$ ,  $K_{AC}$  terms), and the translocation rate constants ( $g_E$ ,  $g_{EAC}$ , and  $g_{EAB}$  terms) are depicted in the reaction cycle in the right panel. Subscripts M and N, denote the M and N sides of the cell membrane (part 1/2 continued on next page). (b) A schematic configuration of the competitive symporter ordered binding transport mechanism of two solutes and the regarding net flux transport equation. In this configuration, the carrier exist in four different states on each side of the membrane. Transport equations are reparametrized and transformed into the general resistance form from Layton model [100]. Dissociation constants ( $K_A$ ,  $K_{AB}$ ,  $K_{AC}$  terms), and the translocation rate constants ( $g_E$ ,  $g_{EAC}$ , and  $g_{EAB}$  terms) are depicted in the reaction cycle in the right panel. Subscripts M and N, denote the M and N sides of the cell membrane. [E] $_C$  is the total number of transporter per unit area of the membrane (part 2/2 continued from previous page).

# 5.2.3. Symport transport mechanism (J<sub>Symporter</sub>):

Symporters are capable of co-transporting two or more solutes against the concentration gradient of one solute or group of solutes (see Fig. 10). This section includes several kinetic models of symporters, namely, symporter slippage, symporter two substrates-

ordered binding model, symporter three substrates-ordered binding model, symporter competitor-ordered binding model, and the symporter simplified model. In the development of these models, it is assumed that the binding and unbinding of the solvent with the carrier on the two surfaces of the membrane is rapid relative to

A general simplified model of symporter with three substrates

$$aA_M + bB_M + cC_M \Longleftrightarrow aA_N + bB_N + cC_N$$

Net Transport Flux from M to N

$$J_{symporter}^{M,N(net)} = P_{symporter} \frac{[A]_M^a [B]_M^b [C]_M^c - [A]_N^a [B]_N^b [C]_N^c}{\left[\alpha^N + 1\right]^a \left[\beta^N + 1\right]^b \left[\gamma^N + 1\right]^c}$$
(1a)

$$J_{A,symporter}^{M,N(net)} = aJ_{symporter}^{M,N(net)}$$
(1b)

$$J_{B,symporter}^{M,N(net)} = bJ_{symporter}^{M,N(net)}$$
(1c)

$$J_{C,symporter}^{M,N(net)} = cJ_{symporter}^{M,N}$$
(1d)

where  $P_{symporter} = [E]_{t}g_{symporter}$  is the membrane permeability to the symporter and its value can be found experi-

The thermodynamic parameters are defined as: 
$$\alpha^M = \frac{[A]_M}{K_A}, \quad \beta^M = \frac{[B]_M}{K_B}, \quad \gamma^M = \frac{[C]_M}{K_C}$$

$$\alpha^N = \frac{[A]_N}{K_A}, \quad \beta^N = \frac{[B]_N}{K_B}, \quad \gamma^N = \frac{[C]_N}{K_C}$$

Fig. 17. Symporter simplified model. The following assumptions are used: (1) the rapid binding and unbinding assumption, (2) the quasi-steady-state assumption, (3) symmetric carrier assumption (similarity for all rate constants), (4) symporter has a single site which bound the transported solute, (5) the transported solute competed for the same binding sites, and (6) finally, the empty symporter does not cross the membrane (there is no slippage of empty carrier).

the translocation step (rapid equilibrium assumption), and that the turnover rate of the carrier-solute complex can be obtained by invoking the quasi-steady-state assumption.

## **Symporter Slippage:**

Fig. 11 depicts a possible model for a symporter with a random binding order and partial slippage during each transport cycle. In this symport system, the carrier, E, can be oriented toward the M surface of the membrane, where either substrate A or B may bind to it to form the complex  $EA_M$  or  $EB_M$ , respectively. Next, these complexes may undergo another association reaction to form the fully loaded carrier-solute complex ( $\it EAB_{\it M}$ ) or they may face the N side of the membrane through a translocation step ( $EA_N$  or  $EB_N$ ). In this configuration, it is assumed that there are no restrictions on the order of binding, and carrier can cross the membrane in all states, i.e., in the empty (E), partially loaded (EA, EB), and fully loaded carrier (EAB) states, with no sequential translocation order. Turner derived the transport equation of fluxes via this transport mechanism in 1982 and Stein reproduced the kinetic scheme in 2012 [131]. Using the Turner model, the turnover rate of an individual symporter is obtained by invoking the quasi-steady-state assumption. Additionally, the binding reactions are assumed to occur much faster than the translocation steps, so that the concentration of the bound carrier can be determined using the dissociation constants ( $K_A$ ,  $K_B$ , and  $K_{BA}$ ). Furthermore, distinct solute dissociation constants for each step are considered, and the translocation rate constants ( $g_E$ ,  $g_{EA}$ ,  $g_{EB}$ , and  $g_{EAB}$ ) are not necessarily equal. The rate of the net outward transport fluxes for A and B can be obtained using equations 55a and 55b, respectively [131]. In these equations, the parameters  $\alpha$ ,  $\beta$ , and R are related to the carrier translocation rate constants and the dissociation constants, and are expressed in terms of experimentally measurable parameters at the bottom of Fig. 11.

# Two-substrate symporter ordered binding models:

Kinetic schemes for sequential binding (ordered binding) cotransport mechanisms involving two solutes are depicted in

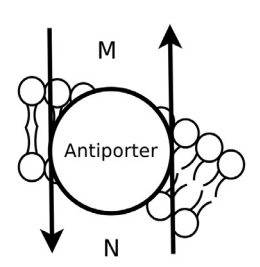
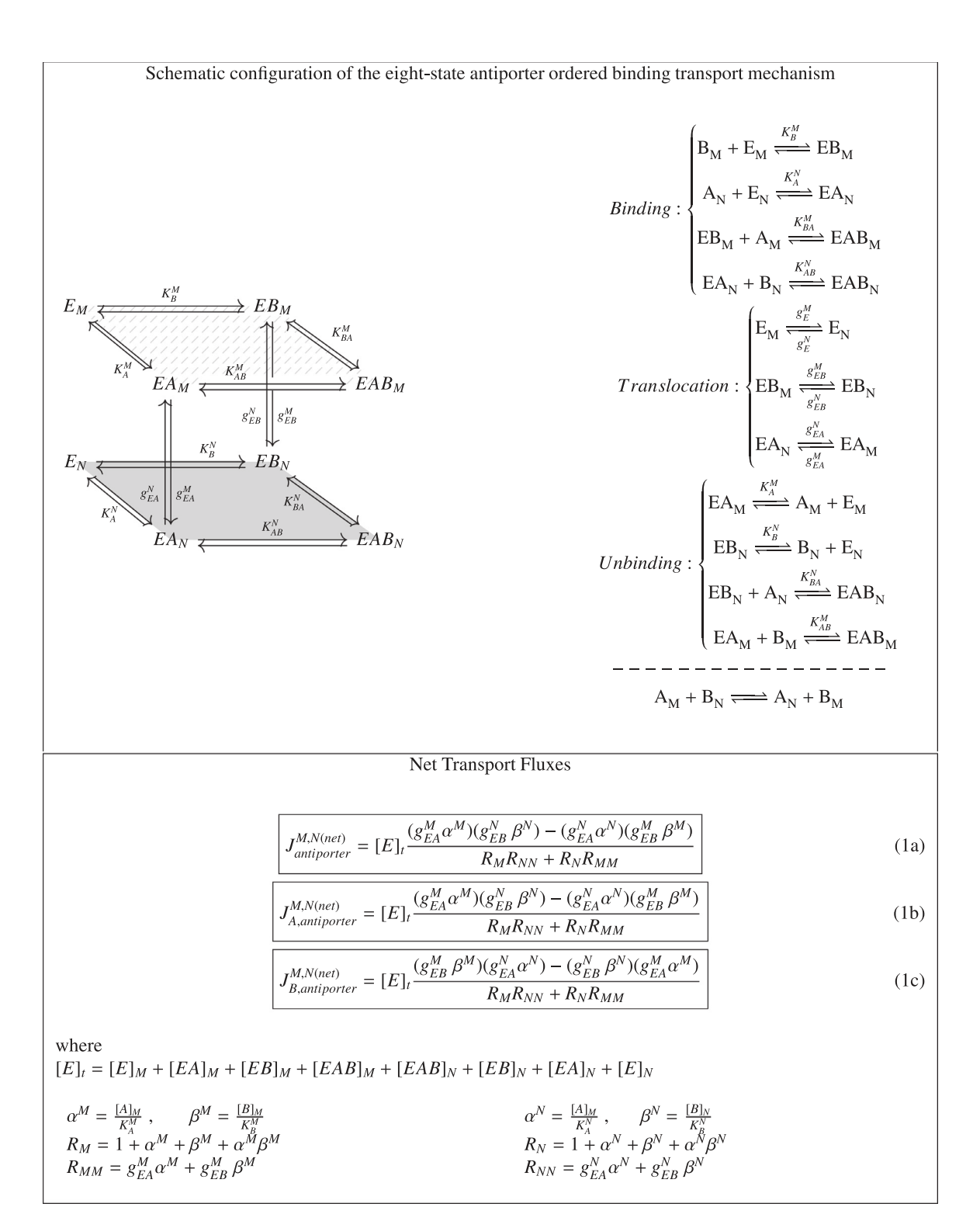


Fig. 18. Antiporter Transport Mechanism.

Figs. 12 and 13. When A binds first, the symport transport mechanism shown in Fig. 13 applies, and the corresponding net flux of A and B through the symporter can be expressed using equations 56b and 56c, respectively. Similarly, the mechanism for the case in which B binds first is illustrated in Fig. 14, and the corresponding net outward flux of A and B can be obtained using equations 57b and 57c, respectively. In these equations,  $J_{symporter}^{M,N(net)}$  is the steadystate turnover rate of the symporter (expressed in equations 56a and 57a, accordingly), and the parameters  $\alpha$ ,  $\beta$ , and R are related to the carrier translocation rate constants and the dissociation constants, which are expressed in terms of experimentally measurable parameters at the bottom of the Figs. 13 and 14, accordingly. These models were developed and parameterized by Stein (2012) [131]. In these models, it is assumed that the partially loaded carriers (EA and EB) cannot translocate at either side of the membrane, and only the fully loaded carrier (EAB) is able to cross the membrane.

## Three-substrate symporter ordered binding model:

Fig. 14 shows a kinetic scheme for a carrier, E, that is capable of transporting molecules of A, B, and C in a ratio of 2A: B: C and exhibits a sequential binding order. In the first step, the carrier faces the M side of the membrane and binds to a molecule of A. After the complex  $EA_M$  is formed, a molecule of B binds to  $EA_M$  to form the  $EAB_M$  complex, followed by the binding of a second molecule



**Fig. 19.** (a) A schematic configuration of the antiporter eight-state transport mechanism and the resulting net transport flux equations. In developing this model, it is assumed that the dissociation constants for binding reactions are not affected by binding of A and B (which means to have  $K_{AB}^{MORN} = K_{B}^{MORN}$  and  $K_{BA}^{MORN} = K_{A}^{MORN}$ ). It is also assumed that: 1) the carrier is non-symmetric and 2) binding reaction occur much faster relative to the translocation of the carrier (rapid binding assumption) (part 1/2 continued on the next page). (b) A schematic configuration of the antiporter eight-state transport mechanism and the resulting net transport flux equations. In developing this model, it is assumed that the dissociation constants for binding reactions are not affected by binding of A and B (which means to have  $K_{AB}^{MORN} = K_{B}^{MORN}$  and  $K_{BA}^{MORN} = K_{A}^{MORN}$ ). It is also assumed that: 1) the carrier is non-symmetric and 2) binding reaction occur much faster relative to the translocation of the carrier (rapid binding assumption) (part 2/2 continued from previous page).

Schematic configuration of the six-state antiporter ordered binding transport mechanism  $\begin{cases} A_M + E_M \xrightarrow{K_A^M} EA_M \mid B_N + E_N \xrightarrow{K_B^N} EB_N \\ & \begin{cases} EA_M \xrightarrow{K_A^M} EA_M \mid B_N + E_N \xrightarrow{K_B^N} EB_N \\ & \begin{cases} EA_M \xrightarrow{g_{EA}^M} EA_N \\ & \end{cases} & \begin{cases} EA_M \xrightarrow{g_{EA}^M} EA_N \\ & \end{cases} \\ & \begin{cases} EA_M \xrightarrow{g_{EA}^M} EB_M \\ & \end{cases} & \begin{cases} EB_M \xrightarrow{K_A^M} EB_M \\ & \end{cases} & \end{cases} \\ & \begin{cases} EA_M \xrightarrow{K_A^M} A_N + E_N \mid EB_M \xrightarrow{K_B^M} B_M + E_M \end{cases} \end{cases}$ 

Net Transport Flux from M to N

$$J_{A,antiporter}^{M,N(net)} = [E]_t \frac{(g_{EA}^M \alpha^M)(g_{EB}^N \beta^N) - (g_{EA}^N \alpha^N)(g_{EB}^M \beta^M)}{R_M R_{NN} + R_N R_{MM}}$$
(1a)

$$J_{B,antiporter}^{M,N(net)} = [E]_{t} \frac{(g_{EB}^{M} \beta^{M})(g_{EA}^{N} \alpha^{N}) - (g_{EB}^{N} \beta^{N})(g_{EA}^{M} \alpha^{M})}{R_{M}R_{NN} + R_{N}R_{MM}}$$
(1b)

where

$$\begin{split} [E]_t &= [E]_M + [EA]_M + [EA]_N + [E]_N + [EB]_N + [EA]_N \\ \alpha^M &= \frac{[A]_M}{K_A^M}, \quad \beta^M = \frac{[B]_M}{K_B^M} \\ R_M &= 1 + \alpha^M + \beta^M \\ R_{MM} &= g_{EA}^M \alpha^M + g_{EB}^M \beta^M \end{split} \qquad \qquad \begin{split} \alpha^N &= \frac{[A]_N}{K_A^N}, \quad \beta^N = \frac{[B]_N}{K_B^N} \\ R_N &= 1 + \alpha^N + \beta^N \\ R_{NN} &= g_{EA}^N \alpha^N + g_{EB}^N \beta^N \end{split}$$

**Fig. 20.** A schematic configuration of the antiporter six-state mechanism of two solutes and the regarding net flux transport equation. Transport equations are reparametrized and transformed into the general resistance form from Weinstein et al. (2000) model [137], the flux equations are transformed to the general form of the resistance terms. In developing this model, it is assumed that the dissociation constants for binding reactions is not affected by binding of *A* and *B* (which means to have  $K_{AB}^{MorN} = K_{A}^{MorN}$  and  $K_{BA}^{MorN} = K_{A}^{MorN} = K_{A}^{MorN}$ ). It is also assumed that: 1) the carrier is non-symmetric and 2) binding reaction occur much faster relative to the translocation of the carrier (rapid binding assumption).

of *A* to form complex *EABA<sub>M</sub>*. Finally, a molecule of C binds to the transporter to give the fully loaded carrier complex *EABAC<sub>M</sub>*. In this model, the carriers can translocate across the membrane in all states (i.e., in the empty, partially loaded, and fully loaded states), and the unbinding reactions occur in the reverse order of binding. This is referred to as a "first on last off" binding order, since the molecule which binds first (e.g., A) on one side of the membrane is the last to unbind from the other side of the membrane. A transport model for this mechanism was first developed by [134]. In this work, the kinetic parameterization method of [131] is followed, and the net outward fluxes of A, B, and C transported through the cotransporter are represented by equations 58a, 58b, and 58c, respectively.

Fig. 15 depicts a different binding/unbinding order for multiple solutes on a carrier. In the scheme, the stoichiometric ratio of the transport reaction is A: 2B: C and the order of binding is as follows: first, solute A binds to the carrier on surface M of the membrane to form the complex  $EA_M$  then the first molecule of B binds to  $EA_M$  to form the complex  $EAB_M$  is formed. This binding is followed by the binding of substrate C and the formation of the complex  $EABC_M$  complex. In the last binding step, the second molecule of B is bound, and the full complex  $(EABCB_M)$  is formed on the M face of the membrane. In this work, the model of the kinetic-transport mechanism is driven by applying

[131] parameterization method, and the overall transport fluxes of A, B, and C are expressed in equations 59b, 59c, and 59d, respectively.

# Competitive symporter ordered binding model:

 $A_M + B_N \Longrightarrow A_N + B_M$ 

Fig. 16 shows a competitive symport transport mechanism involving substrates A, B, and C, in which C competes with B for the same binding sites on the carrier. In the first step, a molecule of A binds to the empty carrier (E), followed by the binding of a B or C molecule to form the complex EAB or EAC, respectively. Next, the formed complexes cross the membrane ( $EAC_N$  or  $EAB_N$ ), where they undergo dissociation reactions in which A unbinds last from both complexes. In this model, it is assumed that the carrier can exist in four different states at each side of the membrane, that only the fully loaded (EAB and EAC) and empty carriers (E) can cross the membrane. The net outward fluxes of B, C, and A can be obtained through equations 60a, 60b, and 60c, respectively. This model can also be applied to the symport transport mechanism of three substrates in a ratio of A: B: C [100].

## Symporter simplified model:

To conclude the section on symporters, a commonly used reduced symporter carrier model is presented (see Fig. 17). In this model, the rapid-equilibrium assumption, quasi-steady-state assumption, and symmetric carrier assumption ( $K_A^M = K_A^N = K_A$ ,  $K_B^M = K_B^N = K_B$ ,  $K_C^M = K_C^N = K_C$ ) are invoked [135]. Furthermore, it is as-

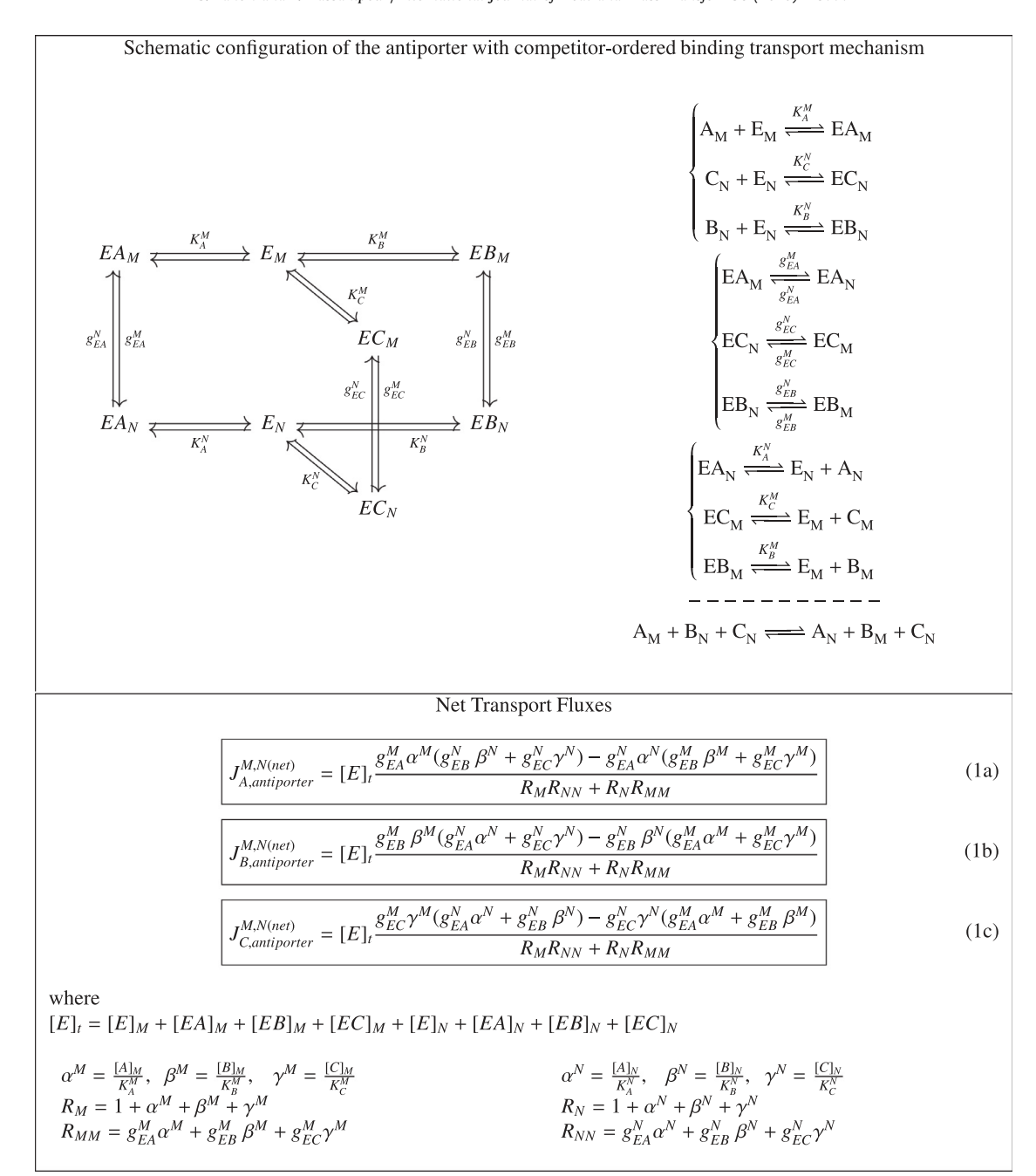


**Fig. 21.** (a) A schematic configuration of the antiporter with competitor-ordered binding transport mechanism of two solutes and the regarding net transport flux equations. In this configuration, the carrier exists in four different states on each side of the membrane. Transport equations are reparameterized to the general model from Layton model [100]. Dissociation constants ( $K_A$ ,  $K_B$ , and  $K_C$  terms), and the translocation rate constants ( $g_{EA}$ ,  $g_{EB}$ , and  $g_{EC}$  terms) are depicted in the reaction cycle in the right panel. Subscripts M and N, denote the M and N sides of the membrane. [E]<sub>t</sub> is the total number of transporter per unit area of the membrane (part 1/2 continued on next page). (b) A schematic configuration of the antiporter with competitor-ordered binding transport mechanism of two solutes and the regarding net transport flux equations. In this configuration, the carrier exists in four different states on each side of the membrane. Transport equations are reparametrized and transformed into the general resistance form from Layton model [100]. Dissociation constants ( $K_A$ ,  $K_B$ , and  $K_C$  terms), and the translocation rate constants ( $g_{EA}$ ,  $g_{EB}$ , and  $g_{EC}$  terms) are depicted in the reaction cycle in the right panel. Subscripts M and N, denote the M and N sides of the membrane. [E]<sub>t</sub> is the total number of transporter per unit area of the membrane (part 2/2 continued from previous page).

sumed the binding and unbinding steps do not follow a particular sequential order. Under these assumptions, for the general case of a symporter transporting three solutes in the ratio of *aA*: *bB*: *cC*, the net outward symporter turnover rate is given by equation 61a and the corresponding solute fluxes of A, B, and C are given by equations 61b, 61c, and 61d, respectively.

# 5.2.4. Antiporter transport mechanism (Jantiporter):

Antiporters, which are also known as exchangers (see Fig. 18), are modeled very similarly to symporters. This section covers several commonly used antiporter models, namely, the eight-state antiporter ordered binding model, six-state antiporter ordered binding model, competitive antiporter ordered-binding model, and simplified antiporter model.

A general simplified antiporter transport with three substrates

$$\boxed{aA_M + bB_N + cC_N \rightleftharpoons aA_N + bB_M + cC_M}$$

Net Transport Flux from M to N

$$J_{antiporter}^{M,N(net)} = P_{antiporter} \frac{(\alpha^M)^a (\beta^N)^b (\gamma^N)^c - (\alpha^N)^a (\beta^M)^b (\gamma^M)^c}{R_M' R_{NN}' + R_N' R_{MM}'}$$
(1a)

$$\overline{J_{A,antiporter}^{M,N(net)}} = aJ_{antiporter}^{M,N(net)}$$
(1b)

$$J_{B,antiporter}^{M,N(net)} = bJ_{antiporter}^{M,N}$$
(1c)

$$\overline{J_{C,antiporter}^{M,N(net)}} = cJ_{antiporter}^{M,N(net)}$$
(1d)

where  $P_{antiporter} = [E]_t g_{antiporter}$  describes the membrane permeability to the antiporter, and the thermodynamic parameters and resistances are defined as:

$$\alpha^{M} = \frac{[A]_{M}}{K_{A}}, \ \beta^{M} = \frac{[B]_{M}}{K_{B}}, \ \gamma^{M} = \frac{[C]_{M}}{K_{C}}$$

$$R'_{M} = (1 + \alpha^{M})^{a} (1 + \beta^{M})^{b} (1 + \gamma^{M})^{c}$$

$$R'_{MM} = (a\alpha^{M} + b\beta^{M} + c\gamma^{M})$$

$$\alpha^{N} = \frac{[A]_{N}}{K_{A}}, \ \beta^{N} = \frac{[B]_{N}}{K_{B}}, \ \gamma^{N} = \frac{[C]_{N}}{K_{C}}$$

$$R'_{N} = (1 + \alpha^{N})^{a} (1 + \beta^{N})^{b} (1 + \gamma^{N})^{c}$$

$$R'_{NN} = (a\alpha^{N} + b\beta^{N} + c\gamma^{N})$$

**Fig. 22.** Antiporter Simplified Model. The following assumptions are used: (1) the rapid binding and unbind assumptions, (2) the quasi-steady-state assumption, (3) similarity assumption for all rate constants (4) antiporter has a single site which bound the transported solute (5) the transported solute competed for the same binding sites (6) finally, the empty antiporter does not cross the membrane.

## Eight-state antiporter ordered binding model:

Fig. 19 shows a scheme of an antiporter transport mechanism in which the substrate A moves from M to N while B is simultaneously transported in the opposite direction. This model is known as the "eight-state" mechanism, as the carrier can exist in eight forms at the two sides of the membrane ( $E_M$ ,  $EA_M$ ,  $EB_M$ ,  $EAB_M$ ,  $E_N$ ,  $EA_N$ ,  $EB_N$  and  $EAB_N$ ). In the first step, the carrier, E, can be facing the M or N side of the membrane, where either solute B or A can bind to the carrier so that the A-carrier complex (EAM) and B-carrier complex  $(EB_N)$  are formed at opposite sides of the membrane. If the translocation of the formed complexes takes place, each of the complexes can undergo either a dissociation reaction or another binding reaction. If the dissociation reaction occurs, solute A will be released from the M face and solute B from the N surface of the membrane. If another binding reaction occurs, the complexes  $EAB_N$  and  $EAB_M$  will be formed at opposite sides of the membrane. Cha et al. (2009) developed a model for eight-state antiporter flux transport equations [136]; here, their model is reparametrized and transformed into the general resistance form. In this model, it is assumed that the dissociation constants for the binding reactions (association reactions) are not affected by the binding of A and B (that is,  $K_{AB}^{MorN} = K_{B}^{MorN}$  and  $K_{BA}^{MorN} = K_{A}^{MorN}$ ). It is also assumed that the carrier is non-symmetric, and that the binding reaction occurs much faster than the translocation steps (rapid binding assumption). Under these assumptions, the antiporter flux can be obtained via equation 62a and the transported fluxes of A and B are given by equations 62b and 62c, respectively.

# Six-state antiporter ordered binding model:

The six-state model is very similar to the eight-state model, except that A and B cannot bind simultaneously to the transporter, and consequently, the formation of the complexes  $EAB_M$  and  $EAB_N$  does not occur. Fig. 20 shows the "ping-pong" model of a six-state antiport transport model. As shown in Fig. 20, in the first step, component A binds to the protein on the outside surface. Assuming

that the binding of solute B to the carrier occurs simultaneously on the other side of the membrane, the A-carrier  $(EA_M)$  and B-carrier  $(EB_N)$  complexes are formed on opposite sides of the membrane. After translocation of the formed complexes, each of the complexes undergoes a dissociation reaction. These dissociation reactions lead to the release of solutes A and B from the N (inside) and M (outside) faces of the membrane, respectively. The A and B fluxes driven from region M to N via this antiport mechanism must be equal and opposite (i.e.,  $J_{B,antiporter}^{M,N} = -J_{A,antiporter}^{M,N}$ ). The six-state model was first developed by Weinstein et al. (2000) [137] under the rapid binding assumption, i.e., the assumption that the solute binding and unbinding reactions at both sides of the membrane occur much faster than the translocation of the carrier complex. In this work, Stein's kinetic parameterization method is applied [131], and the transport fluxes are transformed into the resistance forms. The A and B fluxes are expressed in equations 63a and 63b, respectively.

## Antiporter with competitor-ordered binding model:

Fig. 21 shows a competitive antiporter transport model involving molecules of *A*, *B*, and *C*, in which *C* competes with *B* for the same binding sites on the carrier. In this configuration, *A* flows from the M side to the N side, *B* moves in the opposite direction, and only the loaded carrier can cross the membrane. Here, distinct affinities and dissociation constants at the two sides of the membrane and for each of the solutes are considered, and the forward and backward translocation rate constants of a given solute can differ. In this model, the rapid binding and unbinding assumption and the quasi-steady-state assumption are used. Under these assumptions, the outward fluxes for each of the solutes *A*, *B*, and *C* are obtained by equations 64a, 64b, and 64c, respectively [100].

## Antiporter simplified model:

Simplified models of antiport and symport transporters have been developed using similar assumptions. Sohma et al. (1996) developed a simplified antiporter model for the one-to-one transport of two substrates[138][138]. Here, their model is extended to the general case of an antiporter transporting three solutes in a ratio of aA: bB: cC (see Fig. 22). The following assumptions are used: 1) the rapid binding and unbinding assumption, 2) the quasi-steady-state assumption, and 3) the symmetric carrier assumption (i.e., the velocity constants  $g_{antiporter}$  for transport from the M to the N side of the membrane vice-versa are the same,  $g_{EA}^M = g_{EA}^N = g_{antiporter}$ , and the dissociation constants for each solute on both faces are the same,  $K_A^M = K_A^N = K_A$ ,  $K_B^M = K_B^N = K_B$ , 4) the antiporter has a single binding site for the transported solutes, 5) the transported solutes compete for the same binding sites, and 6) finally, the empty antiporter does not cross the membrane. Using these assumptions, the steady-state turnover rate of the exchanger can be derived from equation 65a, and the corresponding fluxes of substrates A, B, and C are obtained through equations 65b, 65c, and 65d, respectively.

#### 6. Discussion and conclusion

Multiscale mathematical modeling of biological transport mechanisms in the human body has advanced significantly over the last few decades. Simultaneous advances in experimental techniques and computational power have produced models with much greater predictive power, complexity, and usefulness; these models can be used to achieve a more thorough understanding of membrane physiology and disorders. These advances have also led to new techniques in the prevention, diagnosis, and treatment of diseases caused by membrane disorders. This work focused on compiling the mathematical models that have been developed for biological transport in tissue compartments. The tissue volume was divided into five different compartments, including the capillary, interstitial region, cell membrane, intracellular space, and duct lumen. Next, mass transport models for fluids and solutes within and across the walls of these compartments were described. These transport mechanisms include diffusion, convection, migration, and membrane-mediated transport mechanisms (channels, uniporters, ATPase pumps, symporters, and antiporters). One or more of these mass transport mechanisms may occur in each of the five compartments. In capillaries and ducts, convection is the dominant mechanism of solute transport within these compartments [139,140], and filtration (or hindered convection) is the controlling transport mechanism for fluid flow across their walls [141-143]. Transport within the interstitial matrix occurs mainly via the diffusion mechanism. Mass transport across the cell membrane occurs via diffusion, filtration, water channels, various ion channels, and different families of transporters such as pumps, symporters, and antiporters.

The mathematical models describing these transport mechanisms were discussed, and the terminology used for the fundamental concepts of these models was highlighted. The membrane carriers and ion channels were a particular focus. Both detailed and simplified models were provided for the former. Depending on the purpose of the study, one or more of these models can be applied. As discussed earlier, the physics underlying most of these models is similar; the differences among them arise from the binding and unbinding order of the solutes and the assumptions applied for various reaction steps. The basic building blocks of the transport process include the diffusion, convection, and migration mechanisms. These three transport mechanisms occur along an existing gradient (e.g., a pressure, chemical, or electrochemical gradient), and their models require physical parameters such as hydraulic conductance, permeability, diffusion coefficients, viscosity, and mobility. For the convection mechanism, the existing pressure gradients play a controlling role, and the associated parameters are the solute sieving coefficient and hydraulic conductance of the solvent. Diffusion and migration are driven by chemical and electrochemical gradients; the main physical parameters of these processes are the diffusion coefficient and the electrokinetic mobility, respectively. Other transport mechanisms can be expressed as combinations of the main transport mechanisms and using the kinetic reaction equations (the mass-action kinetic, Hill model, and Michaelis-Menten equations); depending on the type of transport, one or more of these equations will be applicable. For example, water channels are modeled as a combination of the diffusion and filtration equations. In the same fashion, the combination of diffusion and migration equations can be used to model the ionic current through the ion channels, which leads to the non-linear Goldman-Hodgkin-Katz model. The linear Ohmic model can also be applied to derive the current through ion channels. In the Ohmic model, the parameters are the membrane electric conductance towards the specific ion of interest and the density of ion channels per unit membrane. Carrier-mediated transport mechanisms are based on a different modeling approach. Since these transporters are fixed within the membrane, they are described merely by using kinetic reaction equations, and the thermal behavior of the transporting molecules is captured in the reaction rate coefficients. These models are experimentally traceable, which allows them to be used as reflective tools for examining the behavior of the transporters and making predictions. Therefore, to model multi-step transporter mechanisms, interpolation of the kinetic data is needed. To facilitate the selection of the appropriate kinetic model for transforming the experimentally obtained kinetic data to the appropriate mathematical model, these transporters were categorized into various groups, and appropriate models for quantitative description of their function were provided.

The development of models at each scale has been achieved by substantial efforts of several established research experts in the interdisciplinary research area of biological mass transport mechanisms. It is not possible to acknowledge or discuss all the research endeavors in different fields in this research area. The comprehensive overview completed in this work represents an attempt to compile the relevant terminology and the developed mass transport mathematical models in biological systems, which have resulted from various lines of research expertise, in a single paper. These contemporary theories and modeling techniques will provide essential knowledge and bridge the gap between physiologists, biophysicists, and engineers interested in modeling biological mass transport processes. Finally, as modeling becomes more prevalent, there is still a need to ensure that the proper physics assumptions are elucidated and considered, and that new modeling methodologies and simplifications are directed towards the key issues. Thus, there remain significant issues that require more research and understanding. While our study was not designed to address the potential issues of currently available models, we hope that researchers can use this work as additional tool to improve the accuracy of the existing models and generate novel models, which in turn could lead to critical discoveries in the important areas of health, pathology, medicine, and membrane disease.

# **Funding**

This work was supported by the National Science Foundation under grant number 1454334.

## **Declaration of Competing Interest**

There are no conflicts of interest to declare.

## **CRediT authorship contribution statement**

**Shadi Zaheri:** Writing - original draft, Conceptualization, Data curation, Formal analysis, Resources. **Fatemeh Hassanipour:** Writing - original draft, Conceptualization, Data curation, Formal analysis, Resources.

### Acknowledgment

The authors would like to thank all the researchers from various fields who have contributed to a better understanding of the biological systems over the past decades.

## Supplementary material

Supplementary material associated with this article can be found, in the online version, at 10.1016/j.ijheatmasstransfer.2020. 119777

#### References

- D. Moulton, V. Sulzer, G. Apodaca, H. Byrne, S. Waters, Mathematical modelling of stretch-induced membrane traffic in bladder umbrella cells, J. Theor. Biol. 409 (2016) 115–132.
- [2] E. Drioli, M. Nakagaki, Membranes and Membrane Processes, Springer Science & Business Media, 2013.
- [3] W. Ang, A.W. Mohammad, Mathematical modeling of membrane operations for water treatment, in: Advances in Membrane Technologies for Water Treatment, Elsevier, 2015, pp. 379–407.
- [4] N.V. Mantzaris, S. Webb, H.G. Othmer, Mathematical modeling of tumor-induced angiogenesis, J. Math. Biol. 49 (2) (2004) 111–187.
- [5] A. Beicha, R. Zaamouche, Mathematical modeling of flux in ultrafiltration membrane, Recent Patents Chem Eng. 5 (2) (2012) 110–115.
- [6] H.S. Silva, A. Kapela, N.M. Tsoukias, A mathematical model of plasma membrane electrophysiology and calcium dynamics in vascular endothelial cells, Am. J. Physiol.-Cell Physiol. 293 (1) (2007) C277–C293.
- [7] R.A. Devenyi, F.A. Ortega, W. Groenendaal, T. Krogh-Madsen, D.J. Christini, E.A. Sobie, Differential roles of two delayed rectifier potassium currents in regulation of ventricular action potential duration and arrhythmia susceptibility, J. Physiol. (Lond.) 595 (7) (2017) 2301–2317.
- [8] M. Ursino, E. Magosso, Acute cardiovascular response to isocapnic hypoxia. i. a mathematical model, Am. J. Physiol.-Heart Circul. Physiol. 279 (1) (2000) H149\_H165
- [9] A.T. Fojo, E.A. Kendall, P. Kasaie, S. Shrestha, T.A. Louis, D.W. Dowdy, Mathematical modeling of "Chronic" infectious diseases: unpacking the black box, in: Open Forum Infectious Diseases, 4, Oxford University Press US, 2017, p. ofx172
- [10] L. Edelstein-Keshet, Mathematical Models in Biology, SIAM, 2005.
- [11] J.D. Murray, Mathematical Biology II, 2, springer, 2002.
- [12] L. Geris, et al., Computational Modeling in Tissue Engineering, Springer, 2013.
- [13] V.C. Rideout, Mathematical and Computer Modeling of Physiological Systems, Prentice Hall Englewood Cliffs, NJ:, 1991.
- [14] W. Stillwell, An Introduction to Biological Membranes: From Bilayers to Rafts, Newnes, 2013.
- [15] P.L. Yeagle, The membranes of cells, Academic Press, 2016.
- [16] J.J. Batzel, M. Bachar, F. Kappel, Mathematical Modeling and Validation in Physiology: Applications to the Cardiovascular and Respiratory Systems, 2064, Springer, 2012.
- [17] J.J. Feher, Quantitative Human Physiology: An Introduction, Academic press, 2017.
- [18] R.I. Macey, Mathematical models of membrane transport processes, in: Physiology of Membrane Disorders, Springer, 1986, pp. 111–131.
- [19] J.P. Keener, J. Sneyd, Mathematical physiology, 1, Springer, 1998.
- [20] S. Motta, F. Pappalardo, Mathematical modeling of biological systems., Brief. Bioinformat. 14 (4) (2013) 411–422, doi:10.1093/bib/bbs061.
- [21] R. Martin, M. Fisher, R. Minchin, K. Teo, A mathematical model of cancer chemotherapy with an optimal selection of parameters, Math. Biosci. 99 (2) (1990) 205–230.
- [22] Z. Liu, C. Yang, A mathematical model of cancer treatment by radiotherapy followed by chemotherapy, Math. Comput. Simul. 124 (2016) 1–15.
- [23] S. Khadraoui, F. Harrou, H.N. Nounou, M.N. Nounou, A. Datta, S.P. Bhat-tacharyya, A measurement-based control design approach for efficient cancer chemotherapy, Inf. Sci. 333 (2016) 108–125.
- [24] H. Moradi, G. Vossoughi, H. Salarieh, Optimal robust control of drug delivery in cancer chemotherapy: a comparison between three control approaches, Comput. Methods Progr. Biomed. 112 (1) (2013) 69–83.
- [25] T. Sund, A mathematical model for counter-current multiplications in the swim-bladder., J. Physiol. (Lond.) 267 (3) (1977) 679–696.
- [26] D.-M. Oh, H.-k. Han, G.L. Amidon, Drug Transport and Targeting, in: Membrane Transporters as Drug Targets, Springer, 2002, pp. 59–88.

- [27] S. Brady, G. Siegel, R.W. Albers, D. Price, Basic neurochemistry: Principles of molecular, cellular, and medical neurobiology, Academic press, 2011.
- [28] M. Almog, A. Korngreen, Is realistic neuronal modeling realistic? J. Neurophysiol. 116 (5) (2016) 2180–2209.
- [29] A. Farghadan, A. Arzani, The combined effect of wall shear stress topology and magnitude on cardiovascular mass transport, Int. J. Heat Mass Transf. 131 (2019) 252–260.
- [30] R. Klabunde, Cardiovascular Physiology Concepts, Lippincott Williams & Wilkins. 2011.
- [31] F.M. Melchior, R.S. Srinivasan, J.B. Charles, Mathematical modeling of human cardiovascular system for simulation of orthostatic response, Am. J. Physiol.-Heart Circulator. Physiol. 262 (6) (1992) H1920–H1933.
- [32] A. Albanese, L. Cheng, M. Ursino, N.W. Chbat, An integrated mathematical model of the human cardiopulmonary system: model development, Am. J. Physiol.-Heart Circulator. Physiol. 310 (7) (2015) H899-H921.
- [33] J. Xi, P.W. Longest, Numerical predictions of submicrometer aerosol deposition in the nasal cavity using a novel drift flux approach, Int. J. Heat Mass Transf. 51 (23–24) (2008) 5562–5577.
- [34] G. Nucci, C. Cobelli, Mathematical models of respiratory mechanics, in: Modeling Methodology for Physiology and Medicine, Elsevier, 2001, pp. 279–304.
- [35] L. Mao, H. Udaykumar, J. Karlsson, Simulation of micro-scale interaction between ice and biological cells, Int. J. Heat Mass Transf. 46 (26) (2003) 5123–5136.
- [36] L.G. Palmer, Epithelial transport in the journal of general physiology, J. Gen. Physiol. 149 (10) (2017) 897–909.
- [37] J.M. Han, V. Periwal, A mathematical model of calcium dynamics: obesity and mitochondria-associated ER membranes, bioRxiv (2018) 477968.
- [38] B. Binder, A. Goede, N. Berndt, H.-G. Holzhütter, A conceptual mathematical model of the dynamic self-organisation of distinct cellular organelles, PLoS ONE 4 (12) (2009) e8295.
- [39] A.K. Babcock, T.Q. Garvey, M. Berman, A mathematical model for membrane transport of amino acid and Na+ in vesicles, J. Membr. Biol. 49 (2) (1979) 157–169.
- [40] J. Mikekisz, J. Gomulkiewicz, S. Miekisz, Mathematical models of ion transport through cell membrane channels, Math. Applicanda 42 (1) (2014) 39–62.
- [41] E. Gin, E.J. Crampin, D.A. Brown, T.J. Shuttleworth, D.I. Yule, J. Sneyd, A mathematical model of fluid secretion from a parotid acinar cell, J. Theor. Biol. 248 (1) (2007) 64–80.
- [42] N. Alaa, H. Lefraich, Computational simulation of a new system modelling ions electromigration through biological membranes, Theor. Biol. Med. Modell. 10 (1) (2013) 51.
- [43] K. Vafai, Handbook of Porous Media, Crc Press, 2015.
- [44] V.R. Voller, A. Brent, C. Prakash, The modelling of heat, mass and solute transport in solidification systems, Int. J. Heat Mass Transf. 32 (9) (1989) 1719–1731.
- [45] W. Liu, G. Zhao, Z. Shu, T. Wang, K. Zhu, D. Gao, High-precision approach based on microfluidic perfusion chamber for quantitative analysis of biophysical properties of cell membrane, Int. J. Heat. Mass Transf. 86 (2015) 869–879.
- [46] K. Cook, A. Marafie, et al., The role of porous media in modeling fluid flow within hollow fiber membranes of the total artificial lung, J. Porous. Media 15 (2) (2012).
- [47] K. Vafai, Porous Media: Applications in Biological Systems and Biotechnology, CRC Press, 2010.
- [48] L. Wang, L.-P. Wang, Z. Guo, J. Mi, Volume-averaged macroscopic equation for fluid flow in moving porous media, Int. J. Heat Mass Transf. 82 (2015) 357–368.
- [49] J.S. Ultman, H. Baskaran, G.M. Saidel, Biomedical Mass Transport and Chemical Reaction: Physicochemical Principles and Mathematical Modeling, John Wiley & Sons. 2016.
- [50] D.A. Nield, A. Bejan, et al., Convection in Porous Media, 3, Springer, 2006.
- [51] R.B. Bird, Transport phenomena, Appl. Mech. Rev. 55 (1) (2002) R1-R4.
- [52] C.G. Hill, T.W. Root, An Introduction to Chemical Engineering Kinetics & Reactor Design, Wiley Online Library, 1977.
- [53] S. Becker, Modeling of Microscale Transport in Biological Processes, Academic Press, 2016.
- [54] J. Pallares, J.A. Ferré, A simple model to predict mass transfer rates and kinetics of biochemical and biomedical Michaelis-Menten surface reactions, Int. J. Heat Mass Transf. 80 (2015) 192–198.
- [55] J.S. Lolkema, D.-J. Slotboom, The hill analysis and co-ion-driven transporter kinetics, J. Gen. Physiol. 145 (6) (2015) 565–574.
- [56] J.N. Weiss, The hill equation revisited: uses and misuses., FASEB J. 11 (11) (1997) 835–841.
- [57] O. Yifrach, Hill coefficient for estimating the magnitude of cooperativity in gating transitions of voltage-dependent ion channels, Biophys. J. 87 (2) (2004) 822–830
- [58] C. Loudon, K. McCulloh, Application of the hagen-poiseuille equation to fluid feeding through short tubes, Ann. Entomol. Soc. Am. 92 (1) (1999) 153–158.
- [59] B. Pirofsky, The determination of blood viscosity in man by a method based on poiseuille's law, J. Clin. Invest. 32 (4) (1953) 292–298.
- [60] S. Singh, L.V. Randle, P.T. Callaghan, C.J. Watson, C.J. Callaghan, Beyond poiseuille: preservation fluid flow in an experimental model, J. Transplant. 2013 (2013).
- [61] R.L. Fournier, Basic transport phenomena in biomedical engineering, CRC press, 2017.
- [62] M. Khakpour, K. Vafai, Critical assessment of arterial transport models, Int. J. Heat Mass Transf. 51 (3–4) (2008) 807–822.

- [63] W. Gösele, C. Alt, Filtration, Ullmann's Encyclopedia Industr. Chem. (2005).
- [64] L. Costanzo, Physiology Cases and Problems, Lippincott Williams & Wilkins, 2012.
- [65] C.J. Geankoplis, Transport Processes and Separation Process Principles:(Includes Unit Operations), Prentice Hall Professional Technical Reference, 2003.
- [66] L. Luo, B. Yu, J. Cai, M. Mei, Symmetry is not always prefect, Int J Heat Mass Transf 53 (21–22) (2010) 5022–5024.
- [67] E.M. Renkin, Filtration, diffusion, and molecular sieving through porous cellulose membranes, J. Gen. Physiol. 38 (2) (1954) 225–243.
- [68] J.S. Schultz, R. Valentine, C.Y. Choi, Reflection coefficients of homopore membranes: effect of molecular size and configuration., J. Gen. Physiol. 73 (1) (1979) 49–60.
- [69] B. Åberg, J.V. Hägglund, A convection-diffusion model of capillary permeability with reference to single-injection experiments, Ups. J. Med. Sci. 79 (1) (1974) 7–17.
- [70] M. Kojic, M. Milosevic, N. Kojic, Z. Starosolski, K. Ghaghada, R. Serda, A. Annapragada, M. Ferrari, A. Ziemys, A multi-scale FE model for convective-diffusive drug transport within tumor and large vascular networks, Comput. Methods Appl. Mech. Eng. 294 (2015) 100–122.
- [71] J. Lu, W.-Q. Lu, A numerical simulation for mass transfer through the porous membrane of parallel straight channels, Int. J. Heat Mass Transf. 53 (11–12) (2010) 2404–2413.
- [72] B. Rippe, M. Townsley, J. Parker, A. Taylor, Osmotic reflection coefficient for total plasma protein in lung microvessels, J. Appl. Physiol. 58 (2) (1985) 436–442.
- [73] L.J. Groome, G.T. Kinasemitz, J.N. Diana, Diffusion and convection across heteroporous membranes: a simple macroscopic equation, Microvasc. Res. 26 (3) (1983) 307–322.
- [74] S.M. Hassanizadeh, Derivation of basic equations of mass transport in porous media, part 2. Generalized Darcy's and Fick's laws, Adv. Water Resour. 9 (4) (1986) 207–222.
- [75] C. Wilke, P. Chang, Correlation of diffusion coefficients in dilute solutions, AlChE J. 1 (2) (1955) 264–270.
- [76] E. Nagy, Basic equations of the mass transport through a membrane layer, Elsevier, 2012.
- [77] P. Bordat, F. Affouard, M. Descamps, F. Müller-Plathe, The breakdown of the Stokes-Einstein relation in supercooled binary liquids, J. Phys. 15 (32) (2003) 5397.
- [78] H.L. Weissberg, Effective diffusion coefficient in porous media, J. Appl. Phys. 34 (9) (1963) 2636–2639.
- [79] H.-h. Chen, H. Shen, S. Heimfeld, K.K. Tran, J. Reems, A. Folch, D. Gao, A microfluidic study of mouse dendritic cell membrane transport properties of water and cryoprotectants, Int. J. Heat Mass Transf. 51 (23–24) (2008) 5687–5694.
- [80] W. Shinoda, Permeability across lipid membranes, Biochimica et Biophysica Acta (BBA)-Biomembranes 1858 (10) (2016) 2254–2265.
- [81] J. Newman, The effect of migration in laminar diffusion layers, Int. J. Heat Mass Transf. 10 (7) (1967) 983–997.
- [82] N. Ibl, Fundamentals of transport phenomena in electrolytic systems, in: Comprehensive Treatise of Electrochemistry, Springer, 1983, pp. 1–63.
- [83] N.J. Yang, M.J. Hinner, Getting across the cell membrane: an overview for small molecules, peptides, and proteins, Site-Specific Protein Label. (2015) 29–53.
- [84] D.L. Nelson, A.L. Lehninger, M.M. Cox, Lehninger Principles of Biochemistry, Macmillan, 2008.
- [85] R. Funk, lon gradients in tissue and organ biology, Biol. Syst. Open Access 2 (2) (2013) 10–4172.
- [86] R. Krämer, C. Ziegler, Membrane Transport Mechanism: 3D Structure and Beyond, 17, Springer Science & Business Media, 2014.
- [87] C. Peracchia, Handbook of Membrane Channels: Molecular and Cellular Physiology, Academic Press, 2012.
- [88] Q. Yan, Membrane Transporters: Methods and Protocols, 227, Springer Science & Business Media, 2003.
- [89] M.A. Hediger, M.F. Romero, J.-B. Peng, A. Rolfs, H. Takanaga, E.A. Bruford, The abcs of solute carriers: physiological, pathological and therapeutic implications of human membrane transport proteins, Pflügers Archiv 447 (5) (2004) 465–468.
- [90] S.G. Dahl, I. Sylte, A.W. Ravna, Structures and models of transporter proteins, J. Pharmacol. Exp. Ther. 309 (3) (2004) 853–860.
- [91] G. Wisedchaisri, S.L. Reichow, T. Gonen, Advances in structural and functional analysis of membrane proteins by electron crystallography, Structure 19 (10) (2011) 1381–1393.
- [92] D.L. Theobald, C. Miller, Membrane transport proteins: surprises in structural sameness, Nature Struct. Mol. Biol. 17 (1) (2010) 2.
- [93] K. Venko, A.R. Choudhury, M. Novič, Computational approaches for revealing the structure of membrane transporters: case study on bilitranslocase, Comput. Struct. Biotechnol. J. 15 (2017) 232–242.
- [94] S.P. Alexander, E. Kelly, N.V. Marrion, J.A. Peters, E. Faccenda, S.D. Harding, A.J. Pawson, J.L. Sharman, C. Southan, J.A. Davies, et al., The concise guide to pharmacology 2017/18: other ion channels, Br. J. Pharmacol. 174 (2017) S195–S207.
- [95] B. Alberts, D. Bray, K. Hopkin, A.D. Johnson, J. Lewis, M. Raff, K. Roberts, P. Walter, Essential Cell Biology, Garland Science, 2015.
- [96] C. Maffeo, S. Bhattacharya, J. Yoo, D. Wells, A. Aksimentiev, Modeling and simulation of ion channels, Chem. Rev. 112 (12) (2012) 6250–6284.

- [97] V. Salari, H. Naeij, A. Shafiee, Quantum interference and selectivity through biological ion channels, Sci. Rep. 7 (2017) 41625.
- [98] S. Yesylevskyy, V. Kharkyanen, Hierarchy of motions and quasi-particles in a simplified model of potassium channel selectivity filter, J. Biol. Phys. 30 (2) (2004) 187–201.
- [99] S.R. Mathur, J.Y. Murthy, A multigrid method for the poisson-nernst-planck equations, Int. J. Heat Mass Transf. 52 (17–18) (2009) 4031–4039.
- [100] A.T. Layton, A. Edwards, Mathematical Modeling in Renal Physiology, Springer, 2014.
- [101] J.D. Stockand, M.S. Shapiro, Ion Channels: Methods and Protocols, 337, Springer Science & Business Media, 2006.
- [102] B. Hille, et al., Ion Channels of Excitable Membranes, 507, Sinauer Sunderland, MA, 2001.
- [103] J. Zheng, M.C. Trudeau, Handbook of Ion Channels, CRC Press, 2015.
- [104] B. Hille, Ionic channels in excitable membranes. current problems and biophysical approaches, Biophys. J. 22 (2) (1978) 283–294.
- [105] A.L. Hodgkin, A.F. Huxley, A quantitative description of membrane current and its application to conduction and excitation in nerve, J. Physiol. (Lond.) 117 (4) (1952) 500–544.
- [106] C.M. Armstrong, The na/k pump, cl ion, and osmotic stabilization of cells, Proc. Natl. Acad. Sci. 100 (10) (2003) 6257–6262.
- [107] C.V. Falkenberg, J.G. Georgiadis, Water and solute active transport through human epidermis: contribution of electromigration, Int. J. Heat Mass Transf. 51 (23–24) (2008) 5623–5632.
- [108] A. Hill, Fluid transport: a guide for the perplexed, J. Membr. Biol. 223 (1) (2008) 1–11.
- [109] K. Takata, T. Matsuzaki, Y. Tajika, Aquaporins: water channel proteins of the cell membrane, Prog. Histochem. Cytochem. 39 (1) (2004) 1–83.
- [110] A. Verkman, Aquaporins in clinical medicine, Annu. Rev. Med. 63 (2012) 303–316.
- [111] M.C. Papadopoulos, S. Saadoun, Key roles of aquaporins in tumor biology, Biochimica et Biophysica Acta (BBA)-Biomembranes 1848 (10) (2015) 2576–2583.
- [112] R.E. Day, P. Kitchen, D.S. Owen, C. Bland, L. Marshall, A.C. Conner, R.M. Bill, M.T. Conner, Human aquaporins: regulators of transcellular water flow, Biochimica et Biophysica Acta (BBA)-General Subjects 1840 (5) (2014) 1492–1506.
- [113] J.M. Carbrey, P. Agre, Discovery of the aquaporins and development of the field, in: Aquaporins, Springer, 2009, pp. 3–28.
- [114] N.C. de Lanerolle, T.-S. Lee, D.D. Spencer, Astrocytes and epilepsy, Neurother-apeutics 7 (4) (2010) 424–438.
- [115] K. Tani, Y. Fujiyoshi, Water channel structures analysed by electron crystallography, Biochimica et Biophysica Acta (BBA)-General Subjects 1840 (5) (2014) 1605–1613.
- [116] K. Alleva, O. Chara, G. Amodeo, Aquaporins: another piece in the osmotic puzzle, FEBS Lett. 586 (19) (2012) 2991–2999.
- [117] O. Kedem, A. Katchalsky, Thermodynamic analysis of the permeability of biological membranes to non-electrolytes, Biochim. Biophys. Acta 27 (1958) 229–246.
- [118] H.Y. Elmoazzen, J.A. Elliott, L.E. McGann, Osmotic transport across cell membranes in nondilute solutions: a new nondilute solute transport equation, Biophys. J. 96 (7) (2009) 2559–2571.
- [119] E. Landis, Exchange of substances through the capillary walls, Handbook Physiol. Circulation II (1963) 961–1034.
- [120] J. Mitchell, R. Schmidt, J. Shepherd, F. Abboud, Handbook of Physiology, Section 2: The Cardiovascular System, vol. 3. peripheral Circulation and Organ Blood Flow, Oxford University Press, 1983.
- [121] S. Barclay, D. Bennett, The direct measurement of plasma colloid osmotic pressure is superior to colloid osmotic pressure derived from albumin or total protein, Intensive Care Med. 13 (2) (1987) 114–118.
- [122] J.S. Schultz, J.D. Goddard, S.R. Suchdeo, Facilitated transport via carrier-mediated diffusion in membranes: part I. Mechanistic aspects, experimental systems and characteristic regimes, AlChE J. 20 (3) (1974) 417–445.
- [123] A.S. Popel, J.D. Hellums, Theory of oxygen transport to tissue, Crit. Rev. Biomed. Eng. 17 (3) (1989) 257.
- [124] E. Cussler, R. Aris, A. Bhown, On the limits of facilitated diffusion, J. Memb. Sci. 43 (2–3) (1989) 149–164.
- [125] J.E. Darnell, H.F. Lodish, D. Baltimore, et al., Molecular Cell Biology, 2, Scientific American Books New York, 1990.
- [126] S.A. Shaikh, P.-C. Wen, G. Enkavi, Z. Huang, E. Tajkhorshid, Capturing functional motions of membrane channels and transporters with molecular dynamics simulation, J. Comput. Theor. Nanosci. 7 (12) (2010) 2481–2500.
- [127] A. Katzir-Katchalsky, P.F. Curran, Nonequilibrium Thermodynamics in Biophysics, Harvard University Press, 1965.
- [128] A. Kleinzeller, D.J. Benos, M.J. Caplan, Cell Biology and Membrane Transport Processes, 41, Academic Press, 1994.
- [129] R. Gaur, L. Mishra, S.K.S. Gupta, Diffusion and transport of molecules in living cells, in: Modelling and Simulation of Diffusive Processes, Springer, 2014, pp. 27–49.
- [130] S.G. Schultz, S. Schultz, Basic Principles of Membrane Transport, 2, CUP Archive, 1980.
- [131] W. Stein, Transport and Diffusion Across Cell Membranes, Elsevier, 2012.
- [132] T.R. Shannon, K.S. Ginsburg, D.M. Bers, Reverse mode of the sarcoplasmic reticulum calcium pump and load-dependent cytosolic calcium decline in voltage-clamped cardiac ventricular myocytes, Biophys. J. 78 (1) (2000) 322–333.

- [133] R. Garay, P. Garrahan, The interaction of sodium and potassium with the sodium pump in red cells, J. Physiol. (Lond.) 231 (2) (1973) 297–325.
- [134] E. Delpire, K.B. Gagnon, Kinetics of hyperosmotically stimulated Na-K-2Cl cotransporter in xenopus laevis oocytes, Am. J. Physiol.-Cell Physiol. 301 (5) (2011) C1074-C1085.
- [135] T. Hartmann, A. Verkman, Model of ion transport regulation in chloride-secreting airway epithelial cells, Integrated description of electrical, chemical, and fluorescence measurements, Biophys. J. 58 (2) (1990) 391-401.

  [136] C.Y. Cha, C. Oka, Y.E. Earm, S. Wakabayashi, A. Noma, A model of Na+/H+ ex-
- changer and its central role in regulation of pH and Na+ in cardiac myocytes, Biophys. J. 97 (10) (2009) 2674-2683.
- [137] A.M. Weinstein, A mathematical model of the outer medullary collecting duct of the rat, Am. J. Physiol.-Renal Physiol. 279 (1) (2000) F24-F45.
- [138] Y. Sohma, M. Gray, Y. Imai, B. Argent, A mathematical model of the pancreatic ductal epithelium, J. Membr. Biol. 154 (1) (1996) 53-67.
- [139] H.W. Florey, The transport of materials across the capillary wall, Q. J. Exp. Physiol. Cognate Med. Sci. 49 (2) (1964) 117–128.

  [140] J. Aroesty, J.F. Gross, Convection and diffusion in the microcirculation, Mi-
- crovasc. Res. 2 (3) (1970) 247-267.
- [141] C. Michel, Fluid exchange in the microcirculation, J. Physiol. (Lond.) 557 (3) (2004) 701-702.
- [142] Y. Himeno, M. Ikebuchi, A. Maeda, A. Noma, A. Amano, Mechanisms underlying the volume regulation of interstitial fluid by capillaries: a simulation study, Integrat. Med. Res. 5 (1) (2016) 11–21.
- [143] D. Zinemanas, R. Beyar, S. Sideman, Relating mechanics, blood flow and mass transport in the cardiac muscle, Int. J. Heat Mass Transf. 37 (1994) 191-205.